iScience, Volume *26*

Supplemental information

Evidence of a possible multicellular life cycle in *Escherichia coli*

Devina Puri, Xin Fang, and Kyle R. Allison

Supplemental Figures

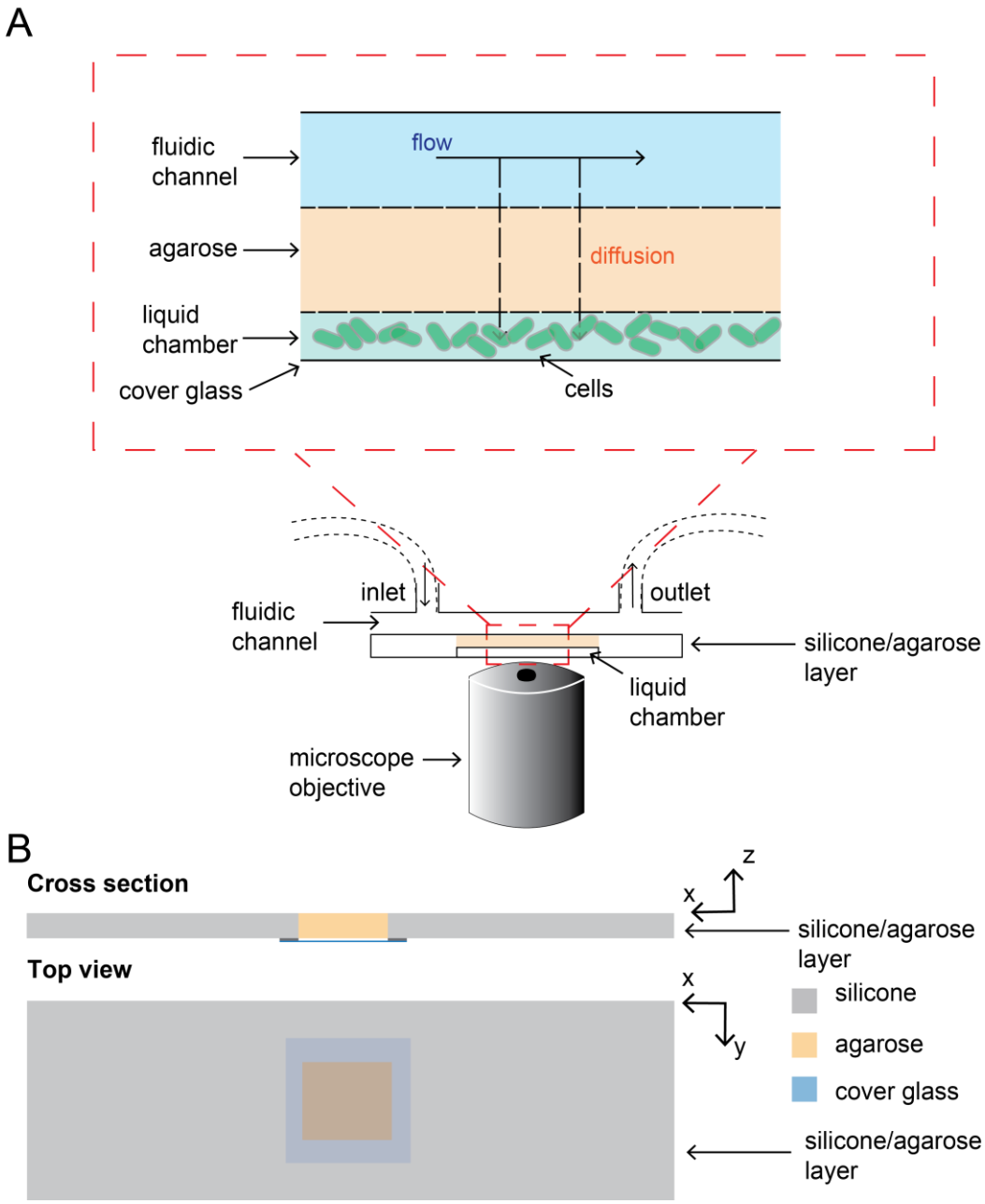

Figure S1. Microfluidic device to track morphogenesis, Related to Figure 1. **(A)** Illustration and working principle of custom microfluidic device to track morphogenesis in hydrostatic growth environment. **(B)** Cross sectional and top view of devices depicting different layers.

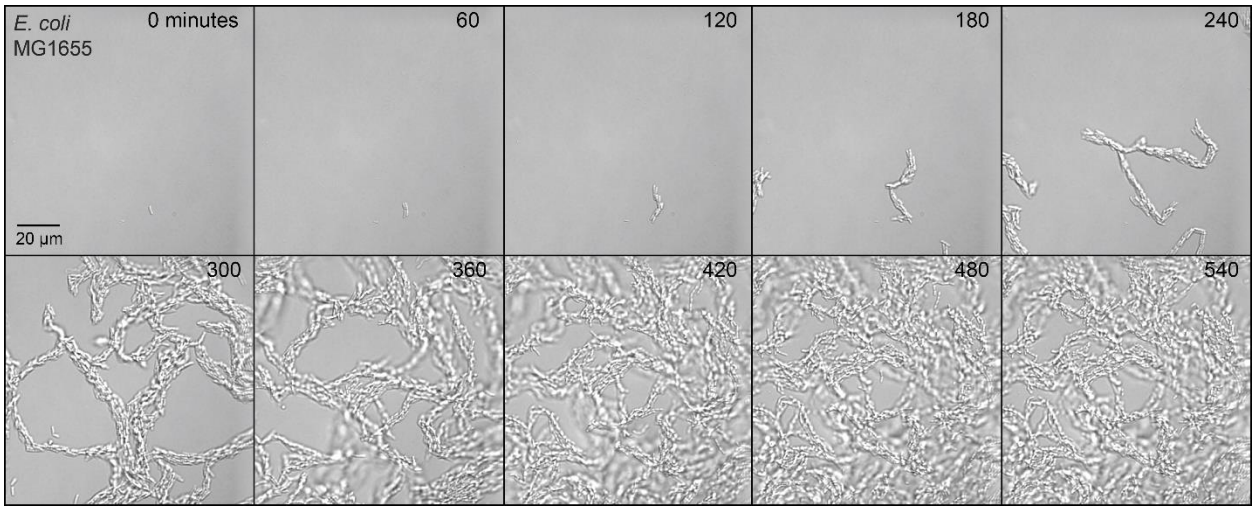

Figure S2. Chain morphogenesis in *E. coli*, Related to Figure 1. Chain morphogenesis in *E. coli* wild-type cells (MG1655), starting from single-cells. Exponential phase cells, grown in LB media, were loaded into microfluidic device set-up depicted in Figure S1 (STAR Methods). Morphogenesis was tracked for ~10 hours at 37 °C. Time and scale are indicated on micrographs.

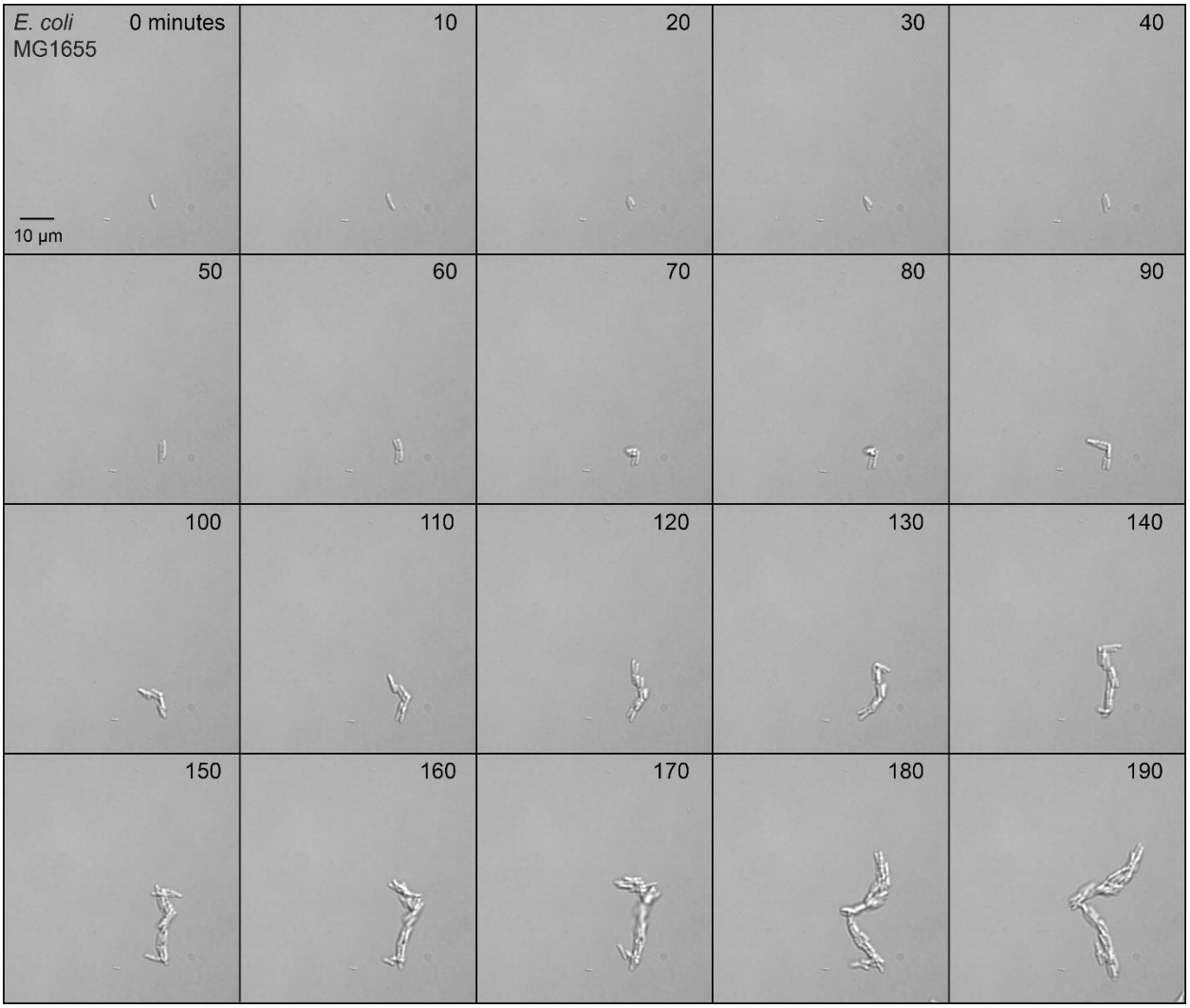

Figure S3. Early stages of chain morphogenesis in *E. coli* wild-type cells, Related to Figure 1. Exponential phase cells, grown in LB media, were loaded into microfluidic device set-up depicted in Figure S1 (STAR Methods). Morphogenesis was tracked for ~10 hours at 37 °C. Time and scale are indicated on micrographs.

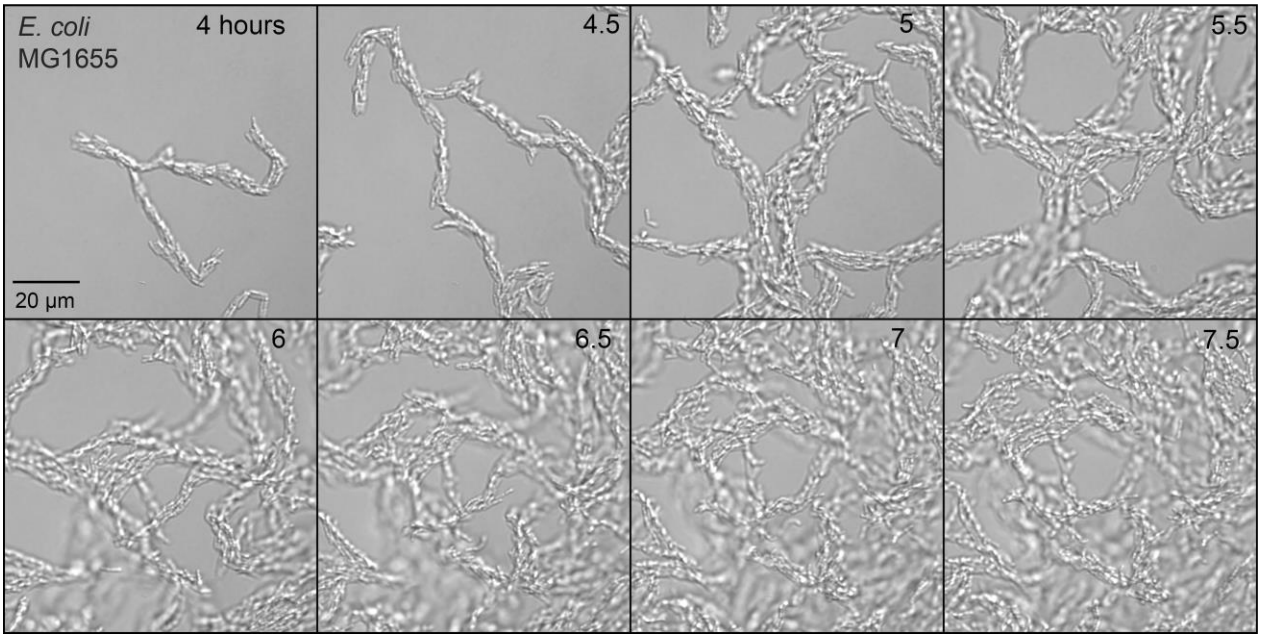

Figure S4. Late stages of chain morphogenesis in *E. coli* wild-type cells, Related to Figure 1. Exponential phase cells, grown in LB media, were loaded into microfluidic device set-up depicted in Figure S1 (STAR Methods). Morphogenesis was tracked for ~10 hours at 37 °C. Time and scale are indicated on micrographs.

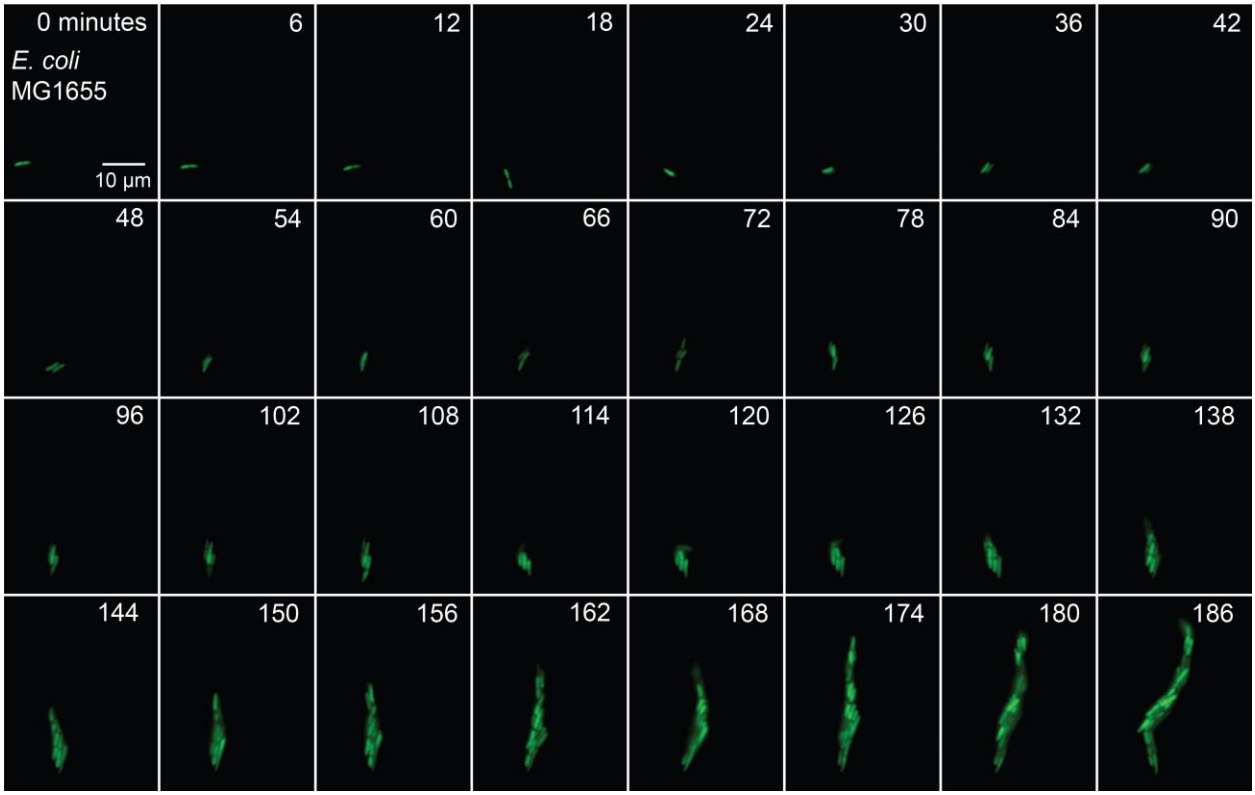

Figure S5. Chain morphogenesis in *E. coli* cells containing green fluorescent protein (GFP), Related to Figure 1. Chain morphogenesis in *E. coli* wild-type cells (MG1655) containing GFP (pUA66-p*ompC*::*gfp*). Exponential phase cells, grown in LB media, were loaded into microfluidic device set-up depicted in Figure S1 (STAR Methods). Morphogenesis was tracked for ~8 hours at 37 °C. Time and scale are indicated on micrographs.

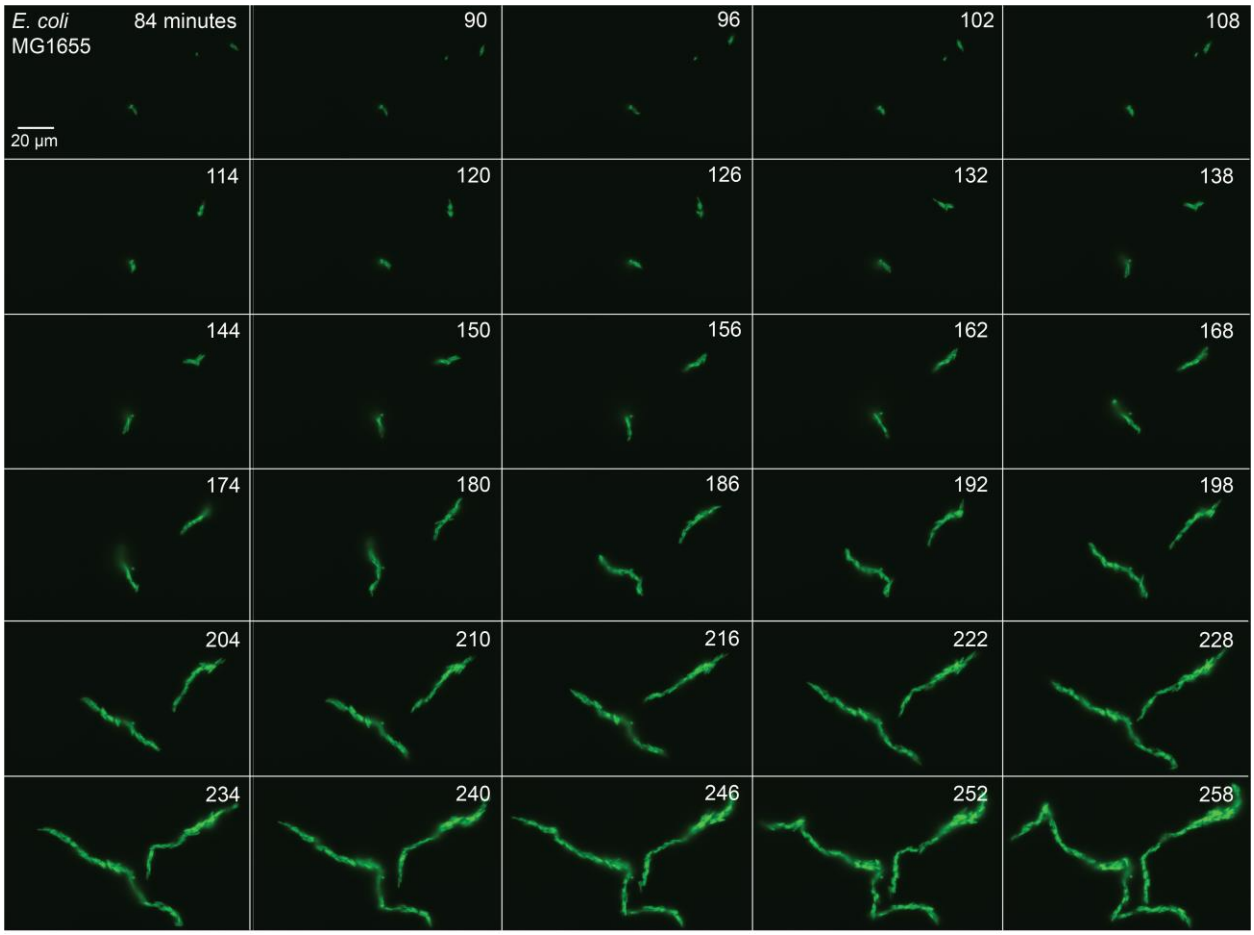

Figure S6. Chain morphogenesis in *E. coli* wild-type cells containing GFP, Related to Figure 1. Exponential phase cells, grown in LB media, were loaded into microfluidic device set-up depicted in Figure S1 (STAR Methods). Morphogenesis was tracked for ~8 hours at 37 °C. Time and scale are indicated on micrographs.

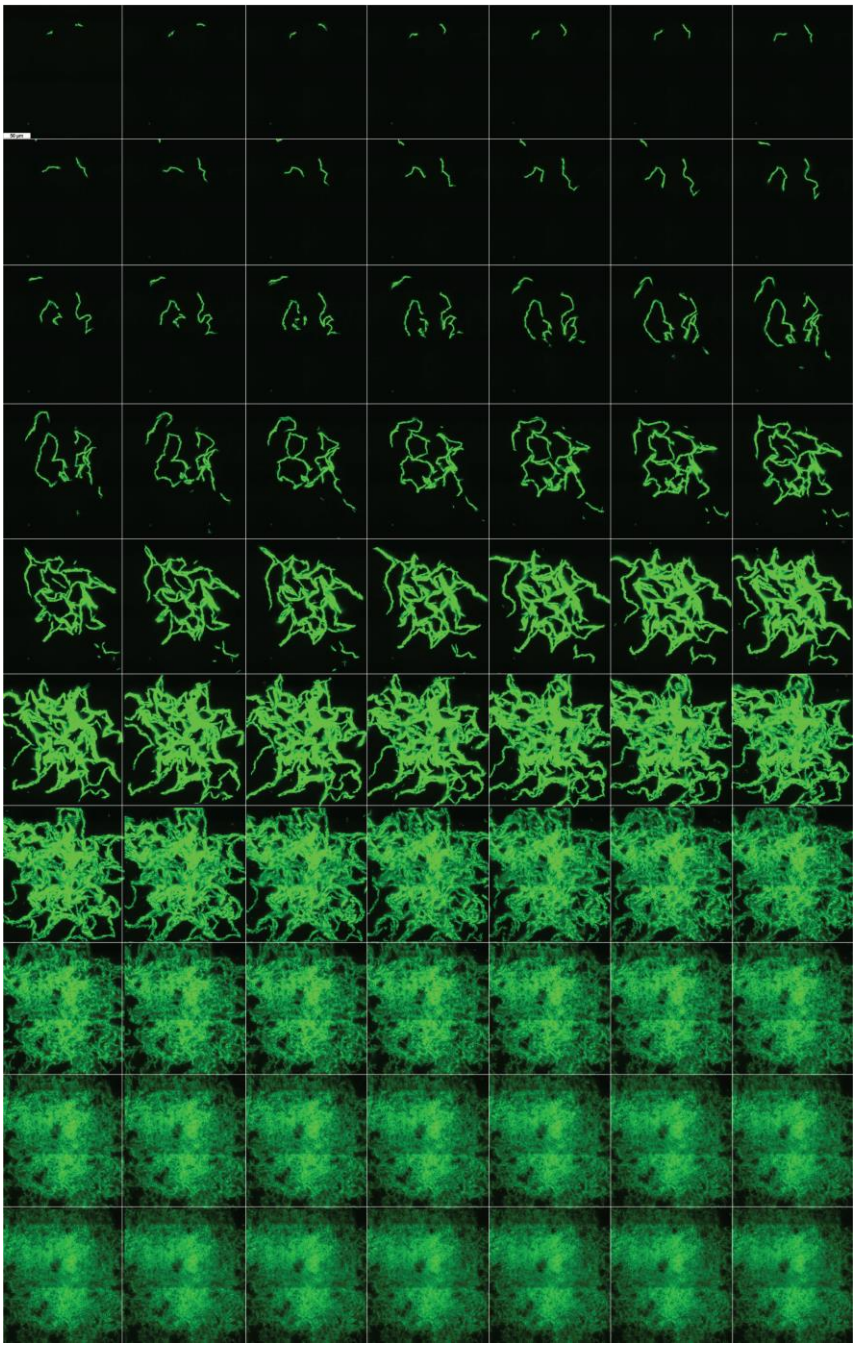

Figure S7. Entire morphogenesis process in *E. coli* wild-type cells containing GFP, Related to Figure 1. Each micrograph was imaged at 6-minute intervals. Scale bar represents 50 μm. Exponential phase cells, grown in LB media, were loaded into microfluidic device set-up depicted in Figure S1 (STAR Methods). Morphogenesis was tracked for ~8 hours at 37 °C.

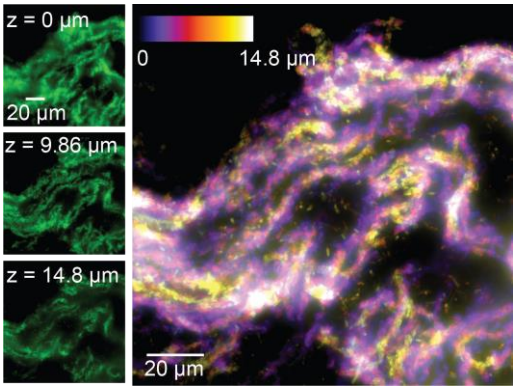

Figure S8. Layered structure of assembled chains visualized through overlaying images collected at different focal planes, Related to Figure 1. Figure represents end-point of chain morphogenesis in *E. coli* cells (containing GFP), tracked in microfluidic device set-up depicted in Figure S1 (STAR Methods) at 37 °C. Z-stack images were captured using green fluorescence channel (with a step height of 1.644 µm) and were overlaid. Color bar used in the figure indicates different heights of the focal planes (z-direction) imaged. Representative examples of individual GFP cross-sectional images collected at different focal planes are displayed in the left panel. Scale is indicated on micrographs.

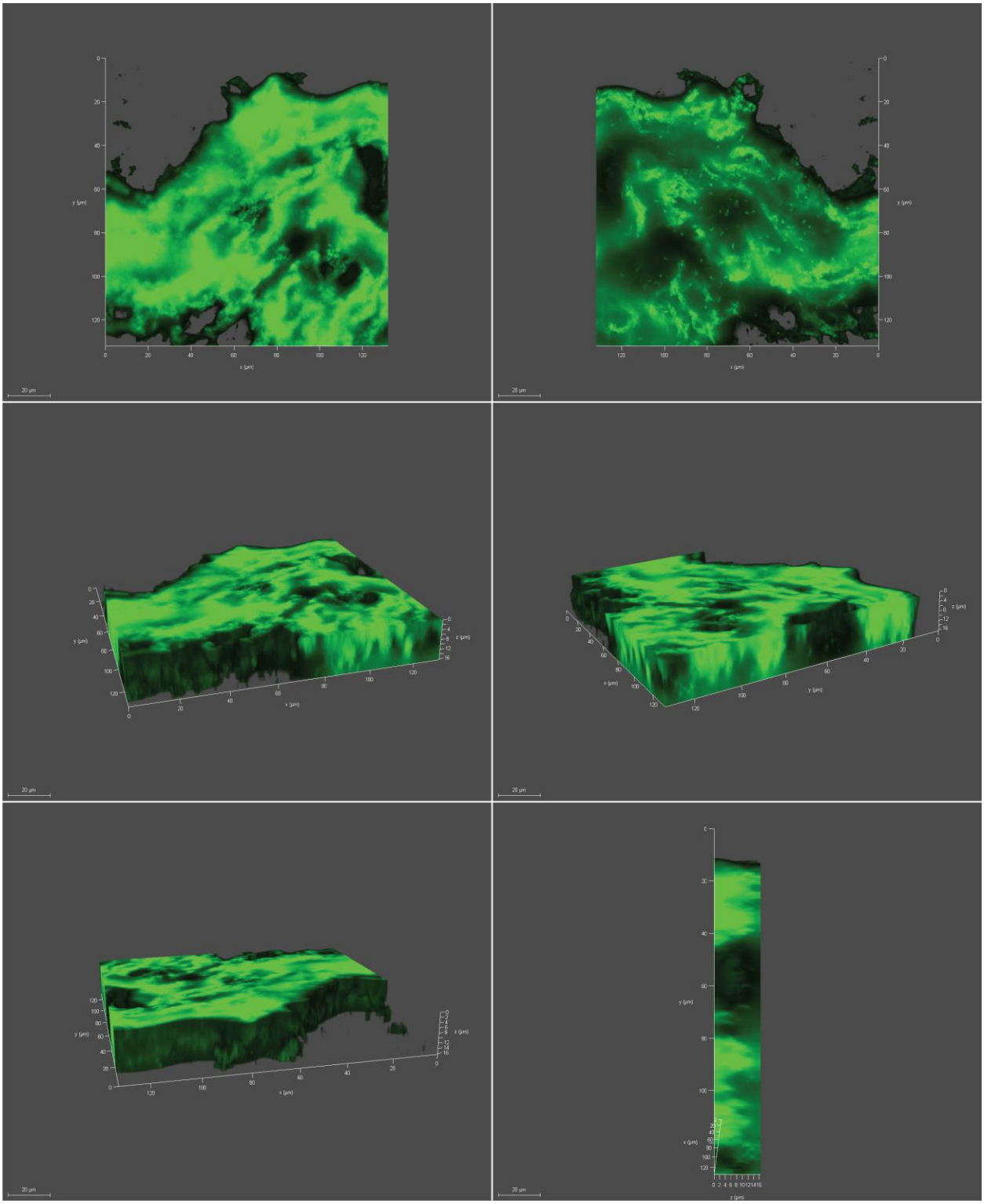

Figure S9. 3D rendering of layered community, Related to Figure 1. 3D rendering of individual z-stack images of layered structure of assembled chains depicted in Figure S8.

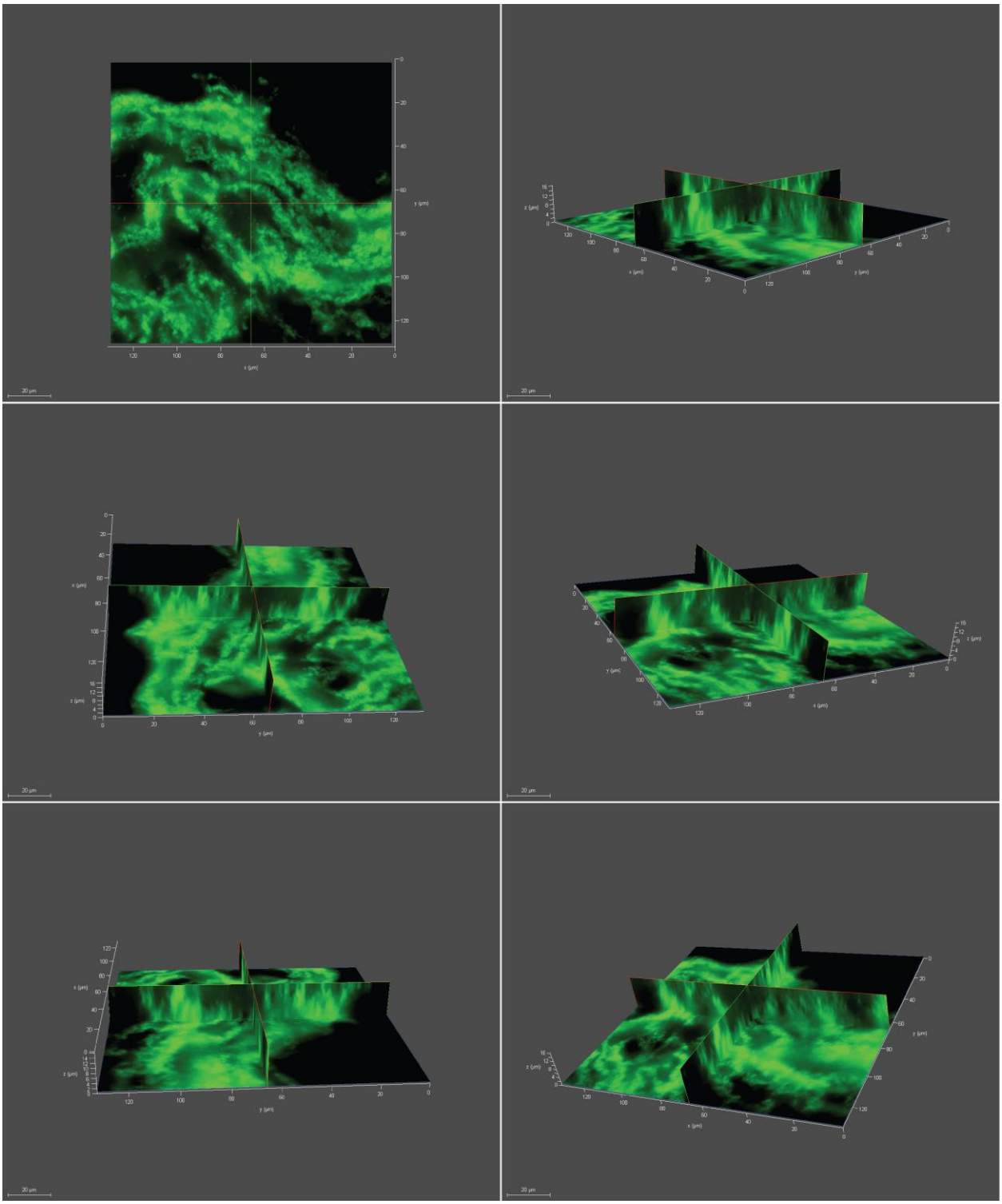

Figure S10. Slice view of 3D rendering of layered community, Related to Figure 1. Slice view of 3D rendered individual z-stack images of assembled chains depicted in S8.

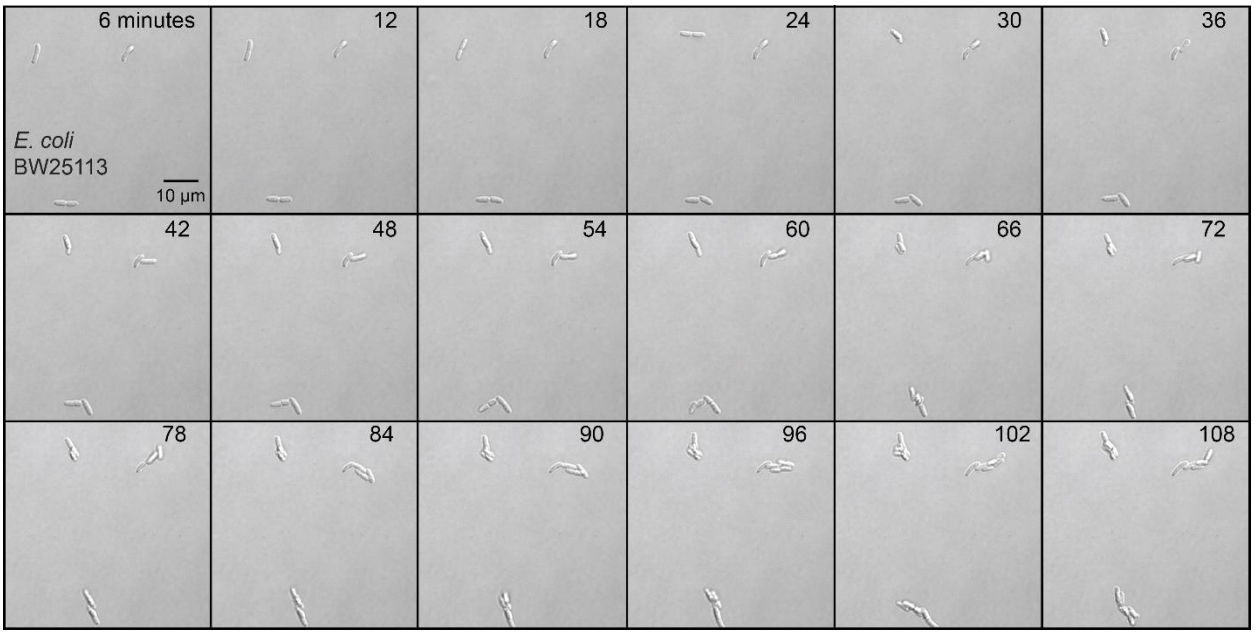

Figure S11. Chain morphogenesis in *E. coli* strain BW25113, Related to Figure 1. Exponential phase cells, grown in LB media at 37 °C, were loaded into microfluidic device set-up depicted in Figure S1 (STAR Methods). Time and scale are indicated on micrographs.

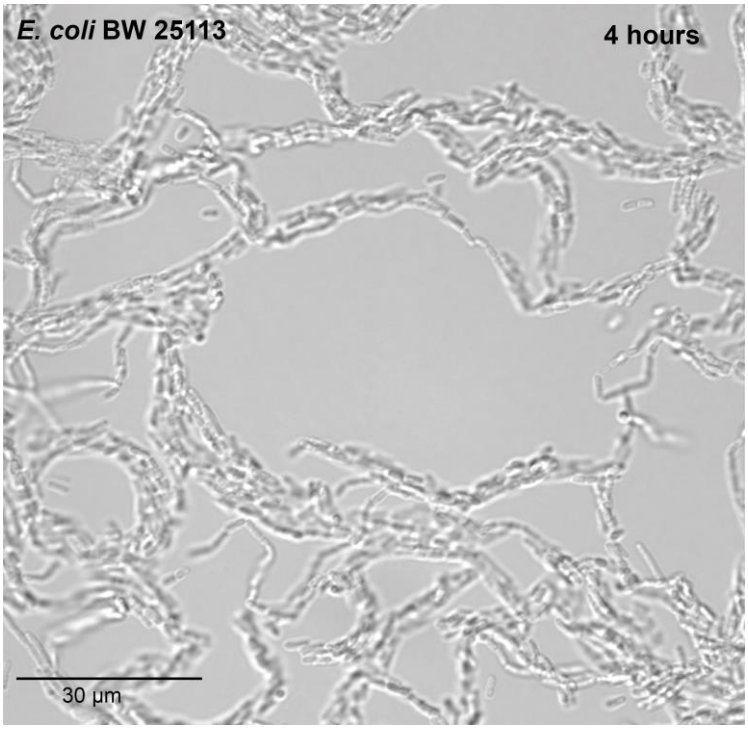

Figure S12. Snapshot of late-stage chain morphogenesis in *E. coli* strain BW25113, Related to Figure 1. Exponential phase cells, grown in LB media, were loaded into microfluidic device set-up depicted in Figure S1 (STAR Methods). Time and scale are indicated on micrograph.

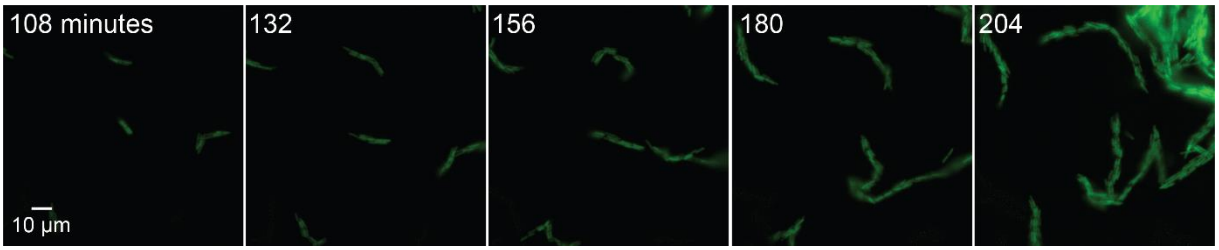

Figure S13. Chain morphogenesis in *E. coli* cells (MG1655) with constitutively expressed green fluorescent protein in EZ rich media, Related to Figure 1. Exponential phase cells grown in EZ rich media at 37 °C were loaded onto microfluidic device set-up depicted in Figure S1 (STAR Methods). Time and scale are indicated on micrograph.

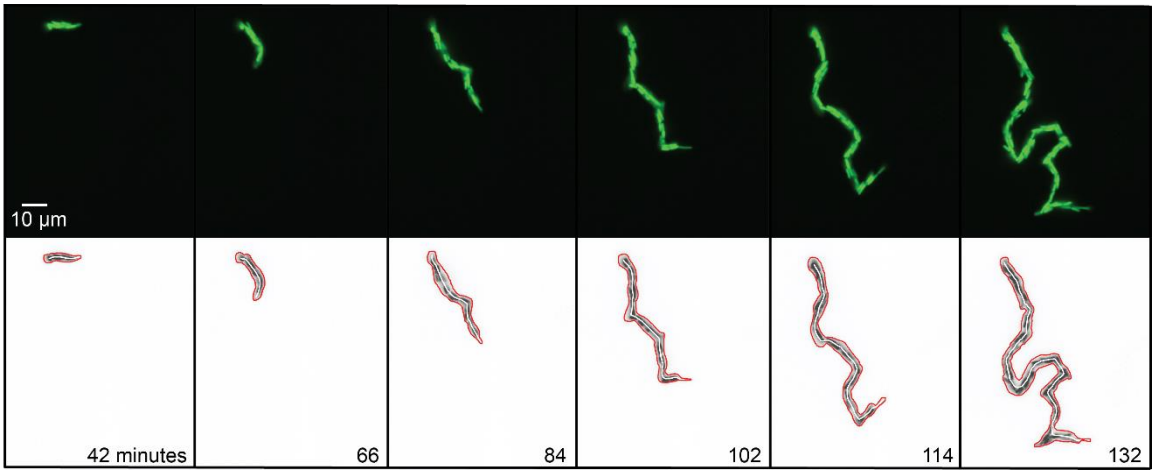

Figure S14. Computational image processing of morphogenetic chains formed by *E. coli* cells (MG1655) containing GFP, Related to Figure 1. Images collected using green fluorescence channel were segmented to calculate boundaries and centerlines, which were used for geometric analysis of chain structures. Lower panel depicts chain centerlines and boundaries overlaid on intensity data. Time and scale illustrated on micrographs.

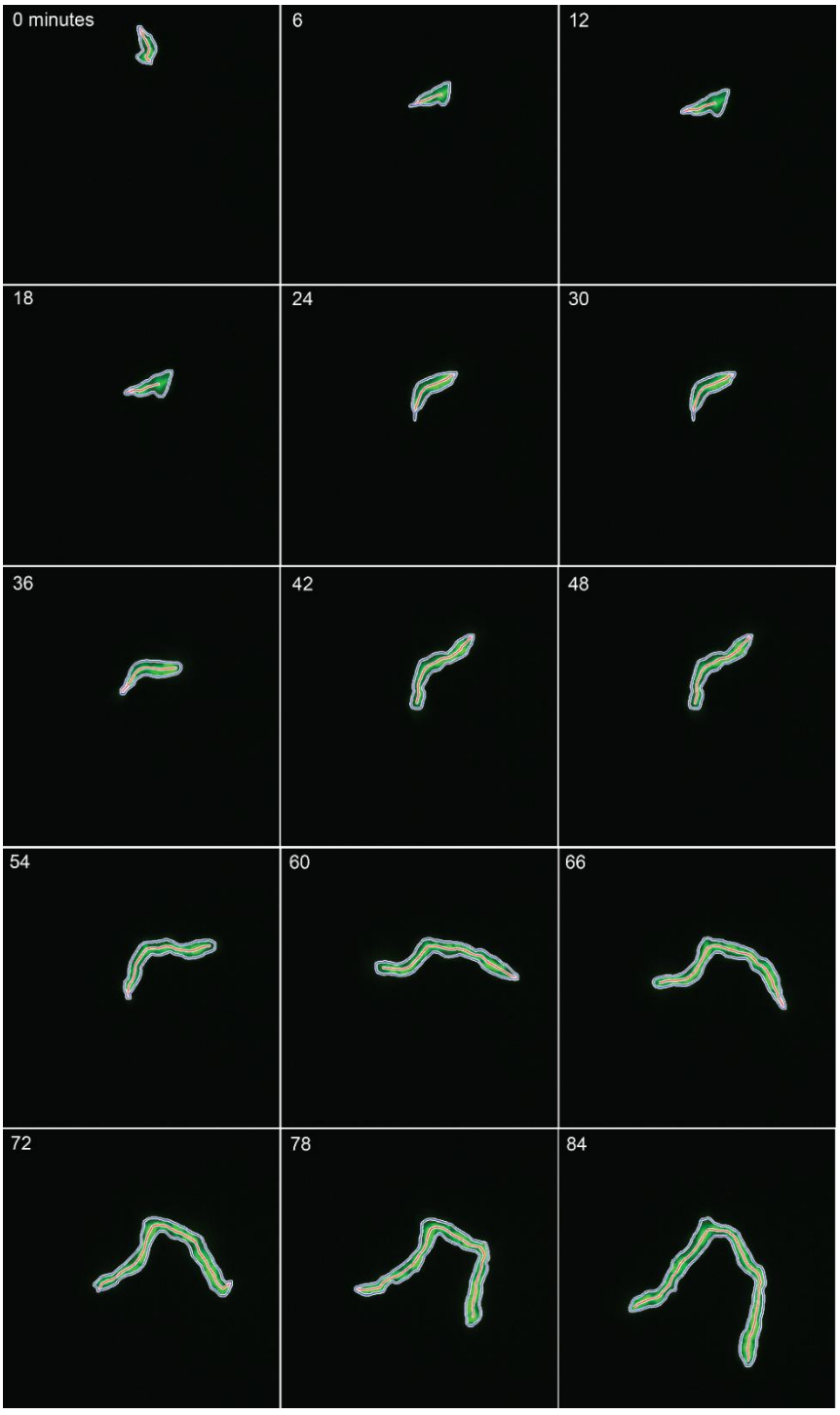

Figure S15. Chain centerlines and boundaries overlaid on GFP data, Related to Figure 1. Exponential phase cells, grown in LB media, were loaded into microfluidic device set-up depicted in Figure S1 (STAR Methods). Micrographs show relative time. Morphogenesis was tracked every 6 minutes.

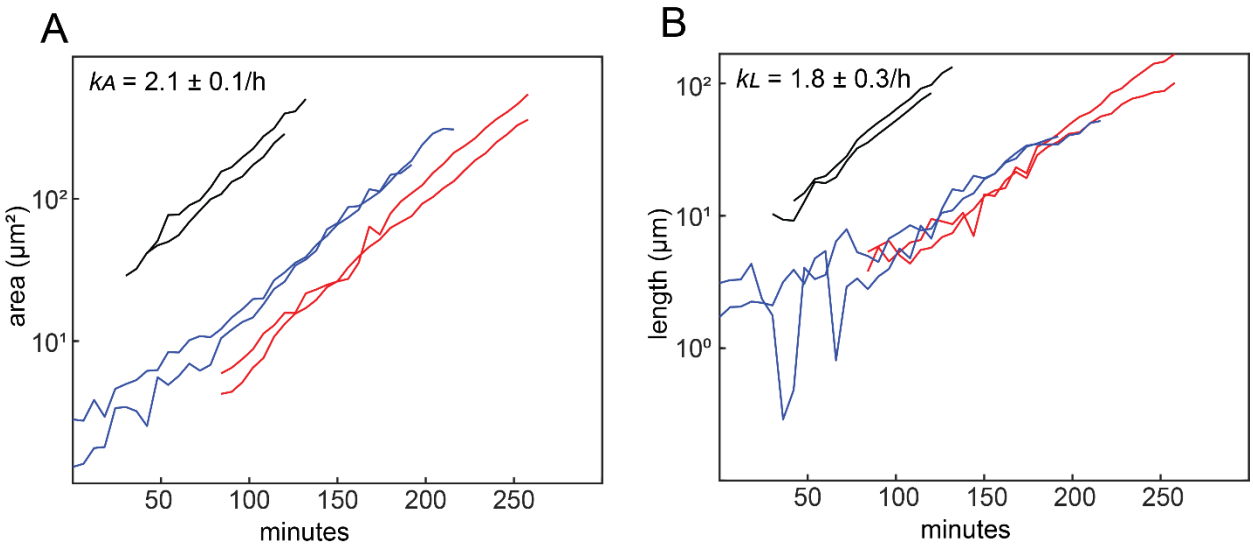

Figure S16. Area and length dynamics during chain morphogenesis, Related to Figure 1. **(A)** Area and **(B)** length dynamics of chains during morphogenesis (colors indicate independent communities tracked within the same experiment). Doubling rate parameters (k_A and k_L) are indicated on plots. Data represent mean ± standard deviation calculated from 6 different chains during morphogenesis.

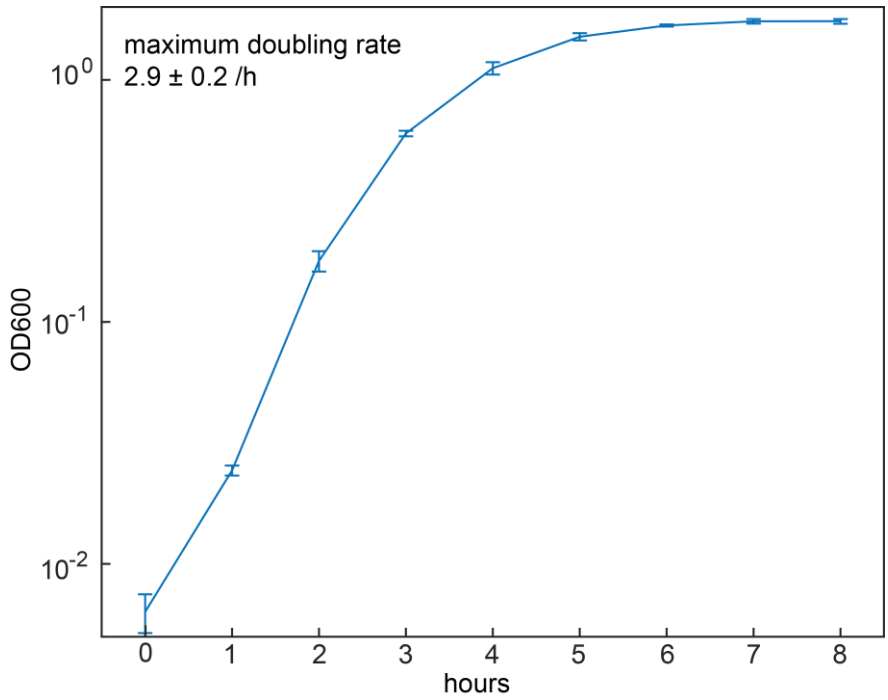

Figure S17. Maximum doubling rate of planktonic cells, Related to Figure 1. Maximum doubling rate of planktonic cells calculated through tracking OD measurements for 8 hours of growth. Data represent mean ± standard deviation (n=3). Maximum doubling rate is indicated on the plot.

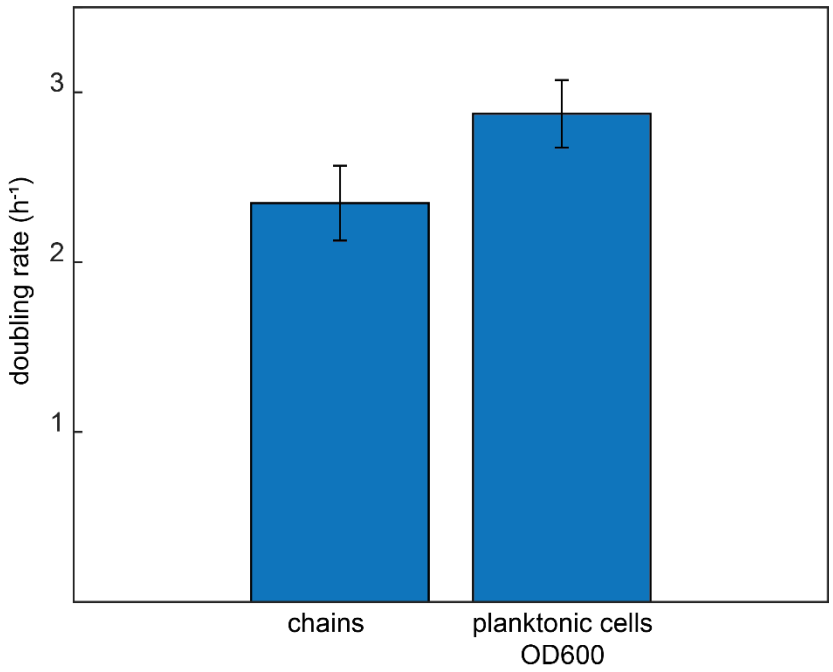

Figure S18. Comparison of doubling rates for cellular chains (area) and planktonic cells (determined by OD measurements; maximum doubling rate), Related to Figure 1. Data represent mean ± standard deviation (n=3).

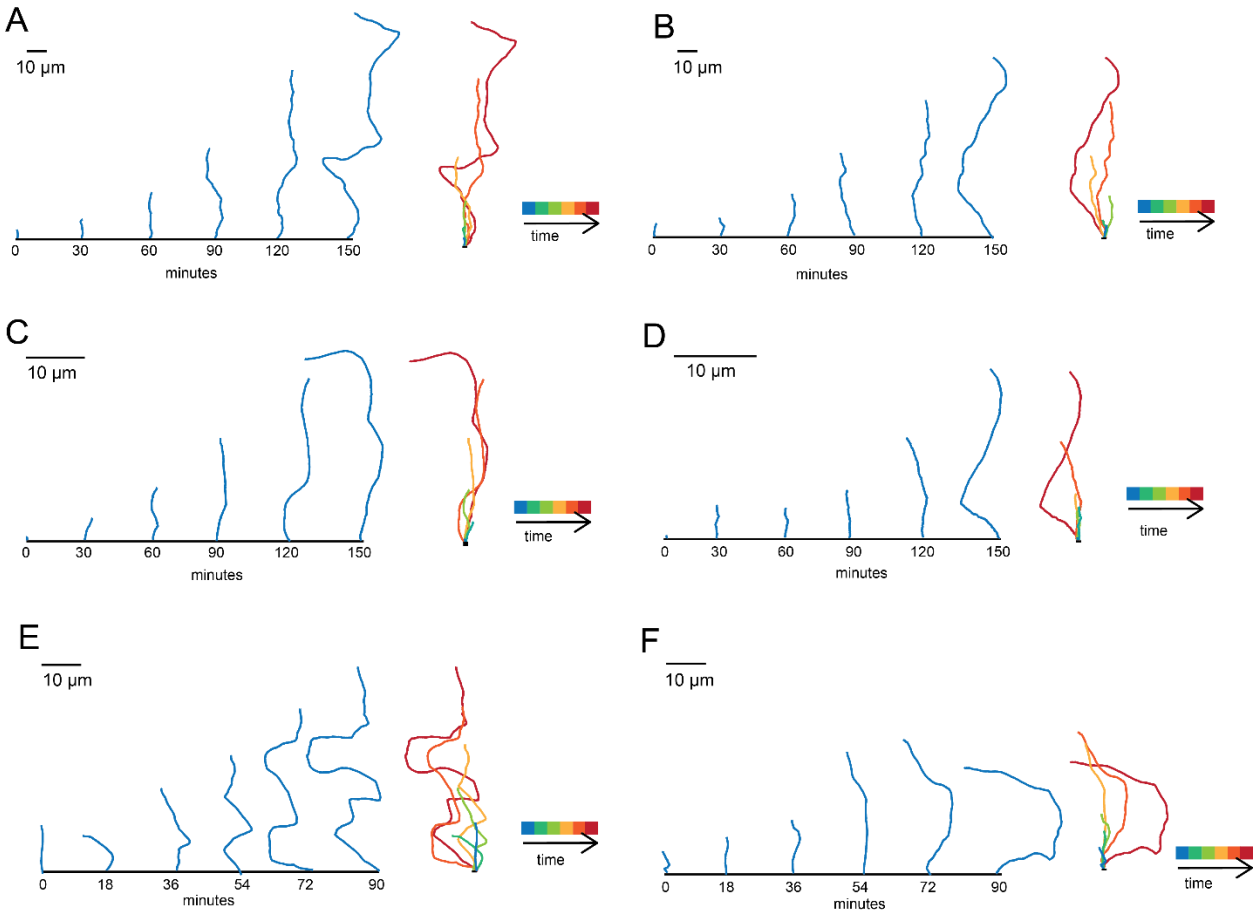

Figure S19. Centerline plots during chain elongation, Related to Figure 1. (left panel) Centerline plots for different time points during *E. coli* chain elongation. Scale bar represents 10 µm. (right panel) Centerline plots overlaid on a single point. Color bar represents time scale. Each set represents dynamics of one cellular chain.

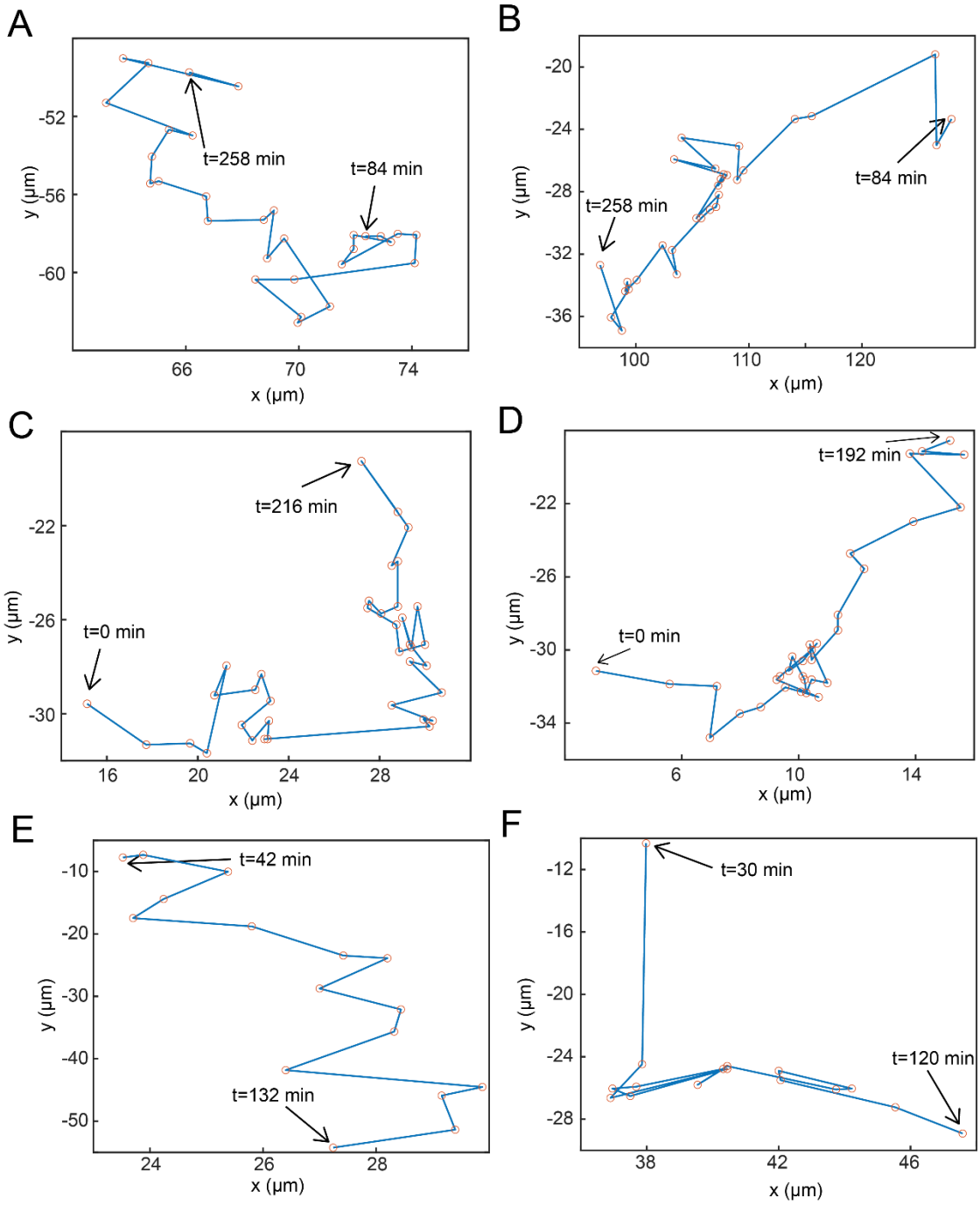

Figure S20. Change in centroid position during elongation of *E. coli* chains, Related to Figure 1. Initial and last time-points are indicated next to centroids of those chains.

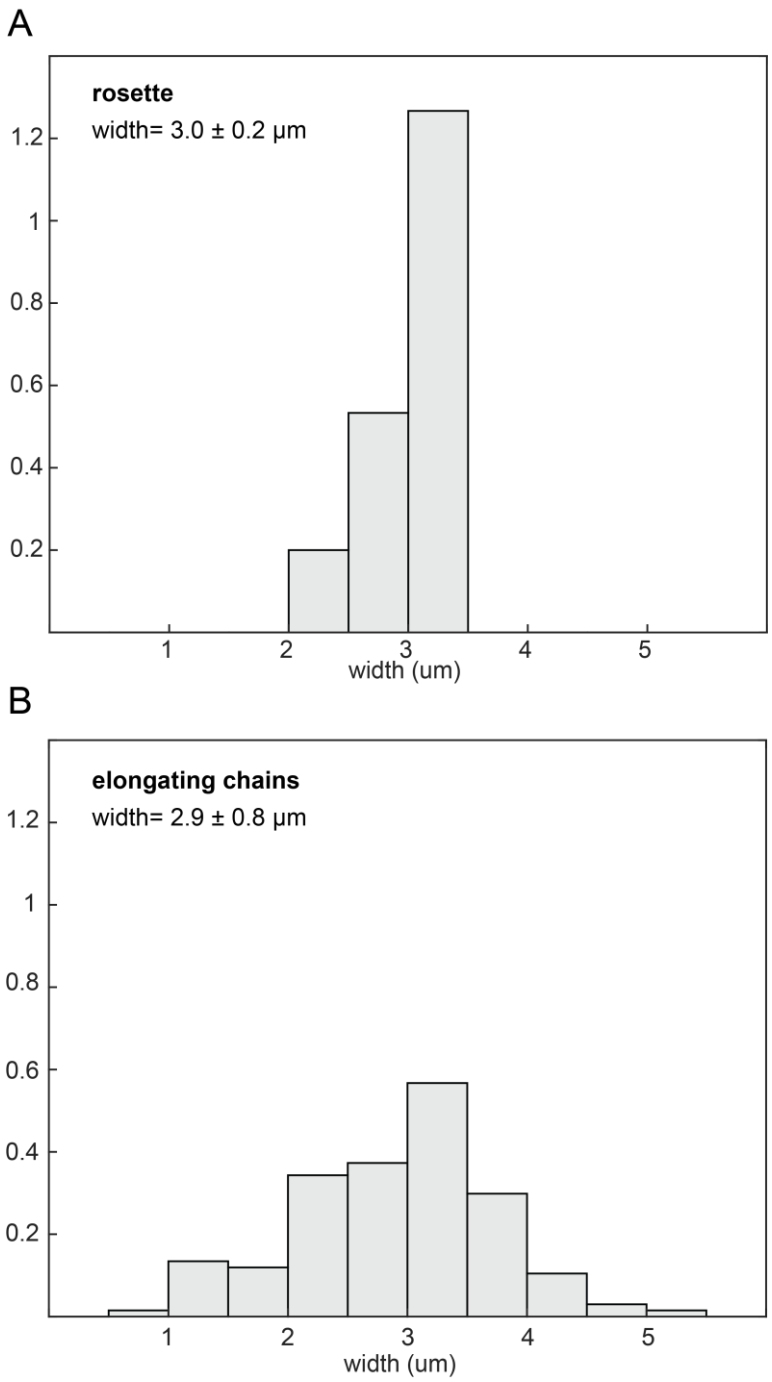

Figure S21. Widths of rosettes and elongating chains, Related to Figure 1. Normalized histograms for widths of **(A)** rosette and **(B)** elongating chains. Widths of elongating chains were calculated for each time point (at 6-minute intervals) during morphogenesis in 6 separate chains. Chain trajectories were tracked for 2-3 hours. All calculated width values were used for the plot (n= 134). Rosette width was determined from 30 width measurements from 10 images (n=30) (STAR Methods). Width values represent mean ± standard deviation.

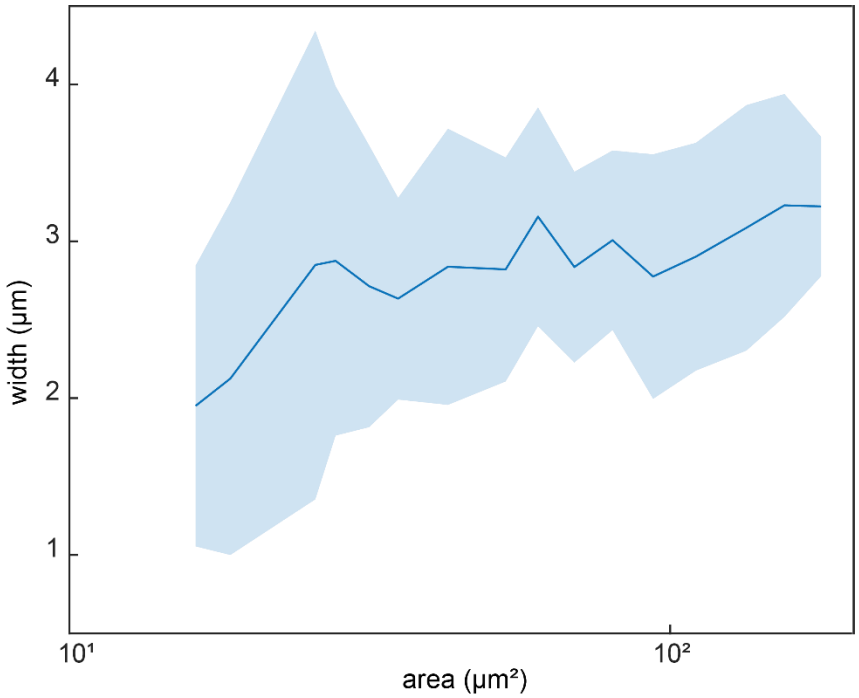

Figure S22. Plot of chain width as a function of chain area during elongation, Related to Figure 1. X-axis represents mean chain area at each time point (at 6-minute intervals) from 6 individual chain trajectories. Data represent mean ± standard deviation (n=6).

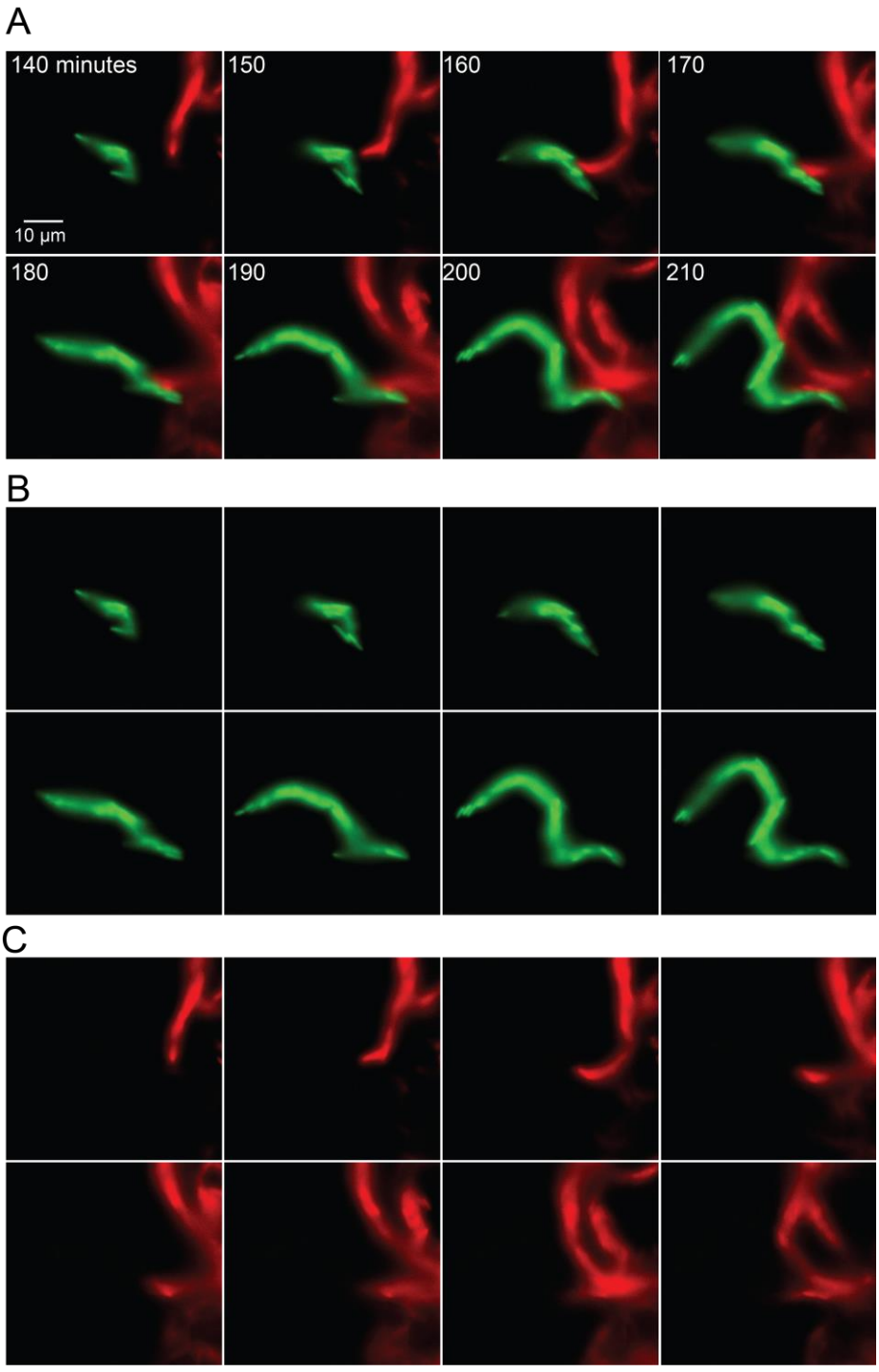

Figure S23. Morphogenesis of wild-type cells containing either GFP (green) or mScarlet (red), Related to Figure 1. **(A)** Morphogenesis of wild-type cells containing either GFP (green) or mScarlet (red) (1:1 ratio). Exponential phase cells, grown in LB media, were loaded into microfluidic device set-up depicted in Figure S1 (STAR Methods). Time and scale indicated on micrograph. Micrographs showing only **(B)** green and **(C)** red channel.

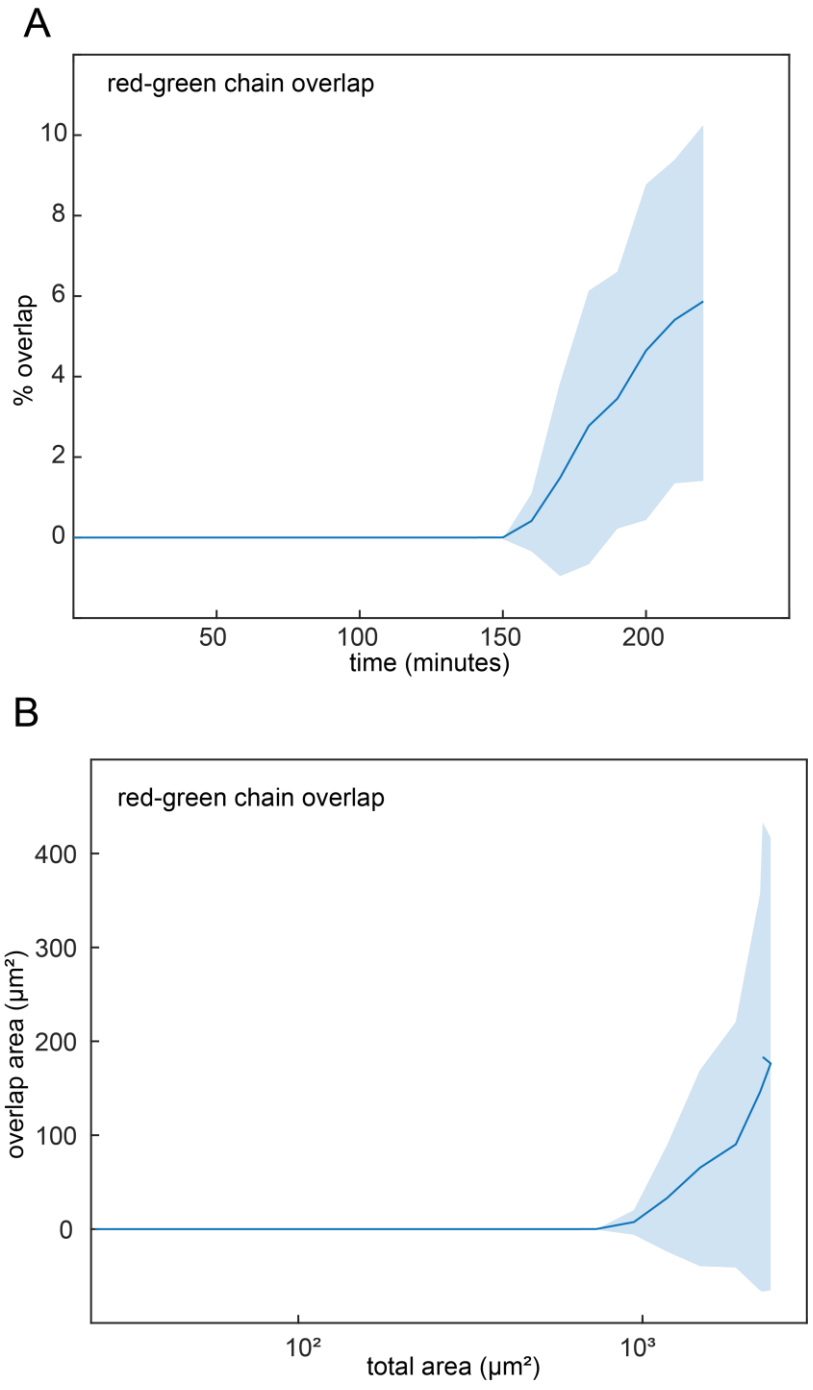

Figure S24. Overlap between red and green chains during morphogenesis, Related to Figure 1. **(A)** Percent overlap between red and green chains during morphogenesis. **(B)** Overlap area of red and green chain as a function of total area. Data represent mean ± standard deviation; n=3. Communities were grown from a mixture of wild-type cells containing either GFP (green) or mScarlet (red) (1:1 ratio), in microfluidic devices depicted in Figure S1 (STAR Methods).

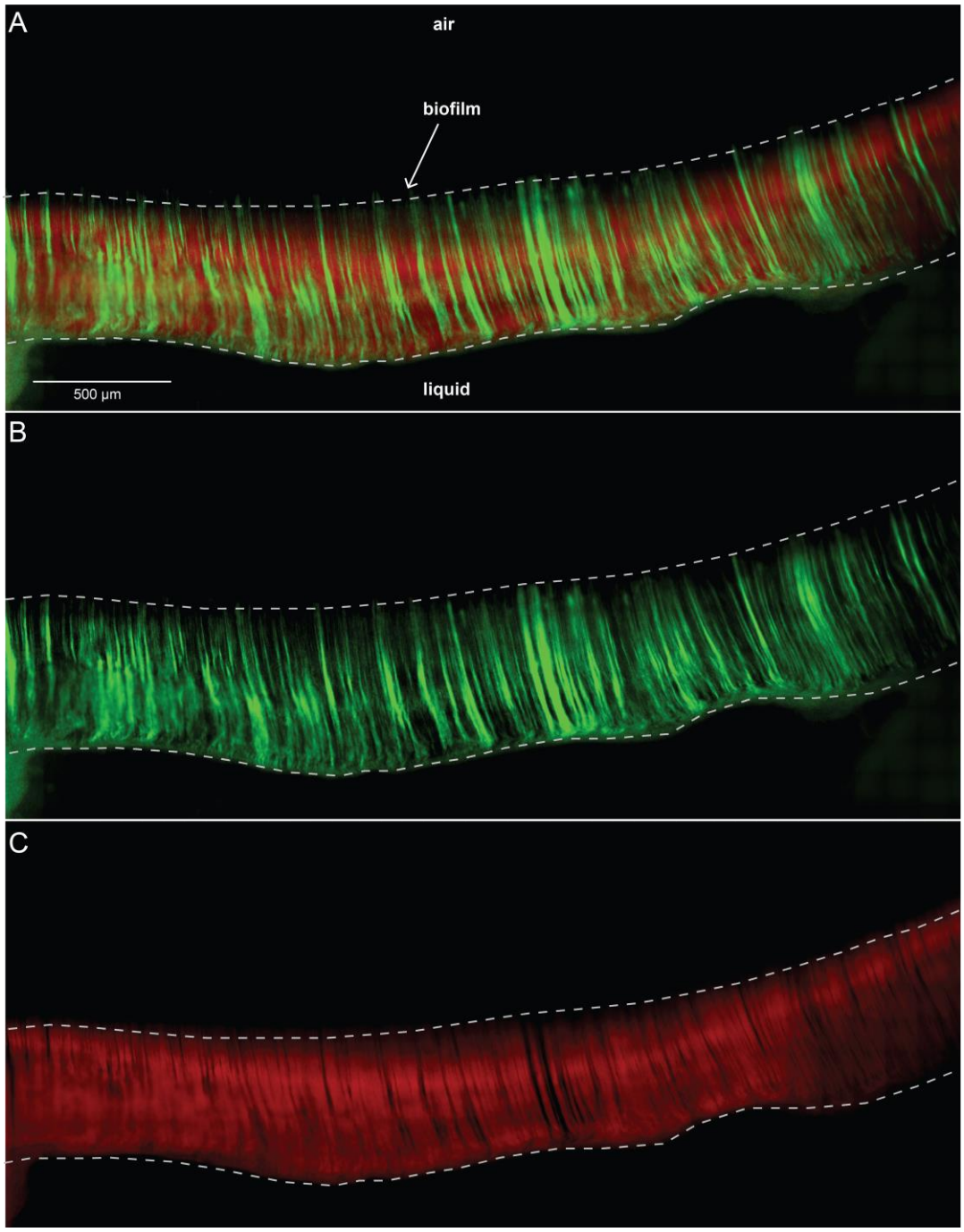

Figure S25. Direct visualization of *E. coli* biofilm in multi-fluorescence, Related to Figure 2. Direct visualization of *E. coli* biofilm imaged in **(A)** multi-fluorescence. Micrographs showing only **(B)** green and **(C)** red channel. Biofilm was grown for 24 hours from a 1:10 mixture of cells containing GFP (green) and mScarlet (red) on cover glass, using method depicted in Figure 2C (STAR Methods). Micrographs represent XY imaging plane. Scale is indicated on micrograph.

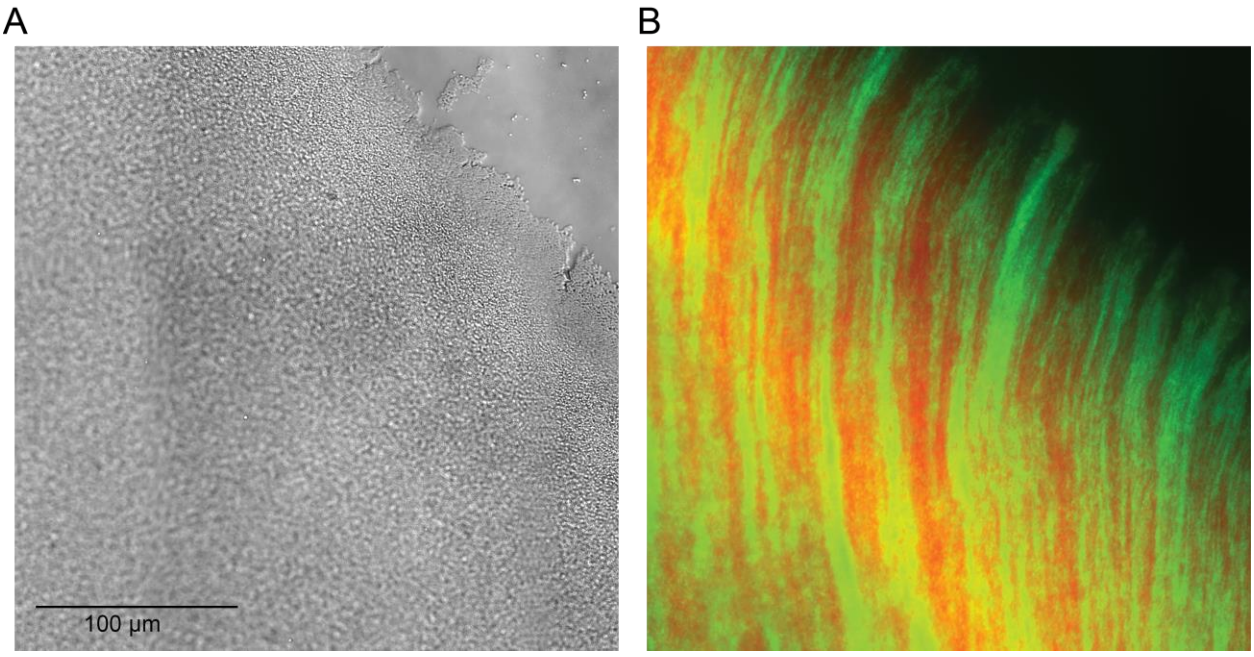

Figure S26. Magnified biofilm regions imaged in bright field and multi-fluorescence, Related to Figure 2. Magnified biofilm regions imaged in **(A)** bright field (DIC) and **(B)** multi-fluorescence. Biofilms were grown from a 1:10 mixture of cells containing GFP (green) and mScarlet (red) on cover glass, using method depicted in Figure 2C (STAR Methods). Scale is indicated on micrograph.

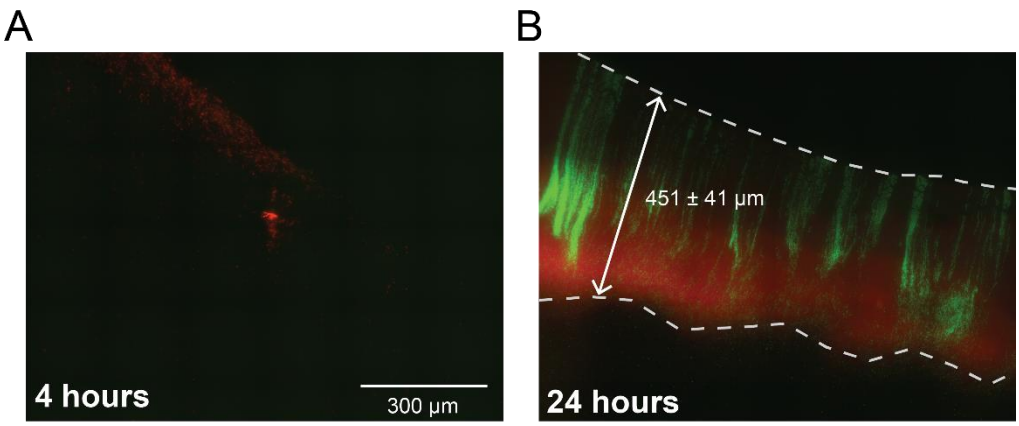

Figure S27. Biofilms grown on cover glass for 4 and 24 hours, Related to Figure 3. Biofilms were grown from a 1:10 mixture of cells containing GFP (green) and mScarlet (red) on cover glass, using method depicted in Figure 2C (STAR Methods), for **(A)** 4 and **(B)** 24 hours. Images for other time-points (8, 12, 16, and 20 hours) are shown in Figure 3A-D. Micrographs represent XY imaging plane. Scale is indicated on micrographs.

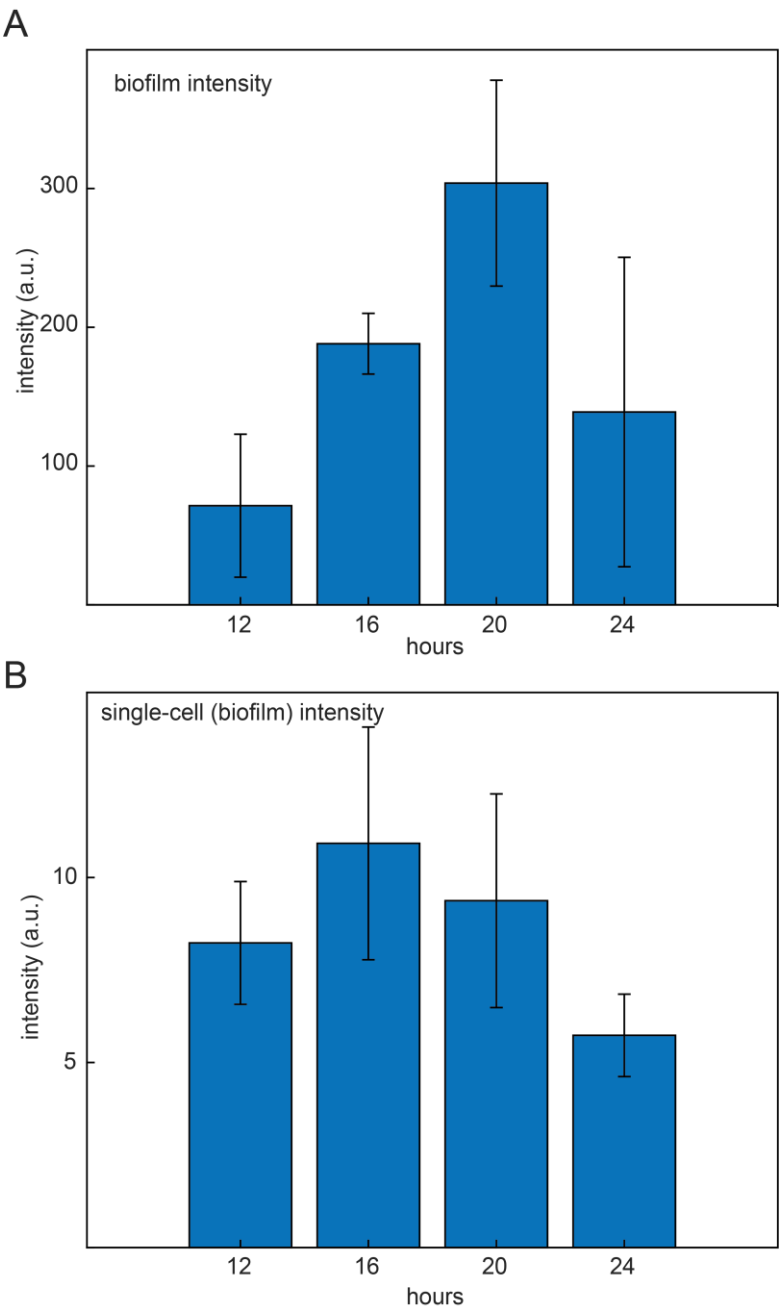

Figure S28. Fluorescence intensity of biofilms at different growth durations, Related to Figure 3. **(A)** Fluorescence intensity of biofilms (red channel) at different growth durations (data represent mean ± standard deviation; n=3). Biofilms were grown from a 1:10 mixture of cells containing GFP (green) and mScarlet (red) on cover glass, using method depicted in Figure 2C (STAR Methods). **(B)** Intensity of individual cells liberated from biofilms at different growth durations (data represent mean ± standard deviation; n=6). Decrease in biofilm intensity at 24 hours was consistent with decline in cell fluorescence at this time.

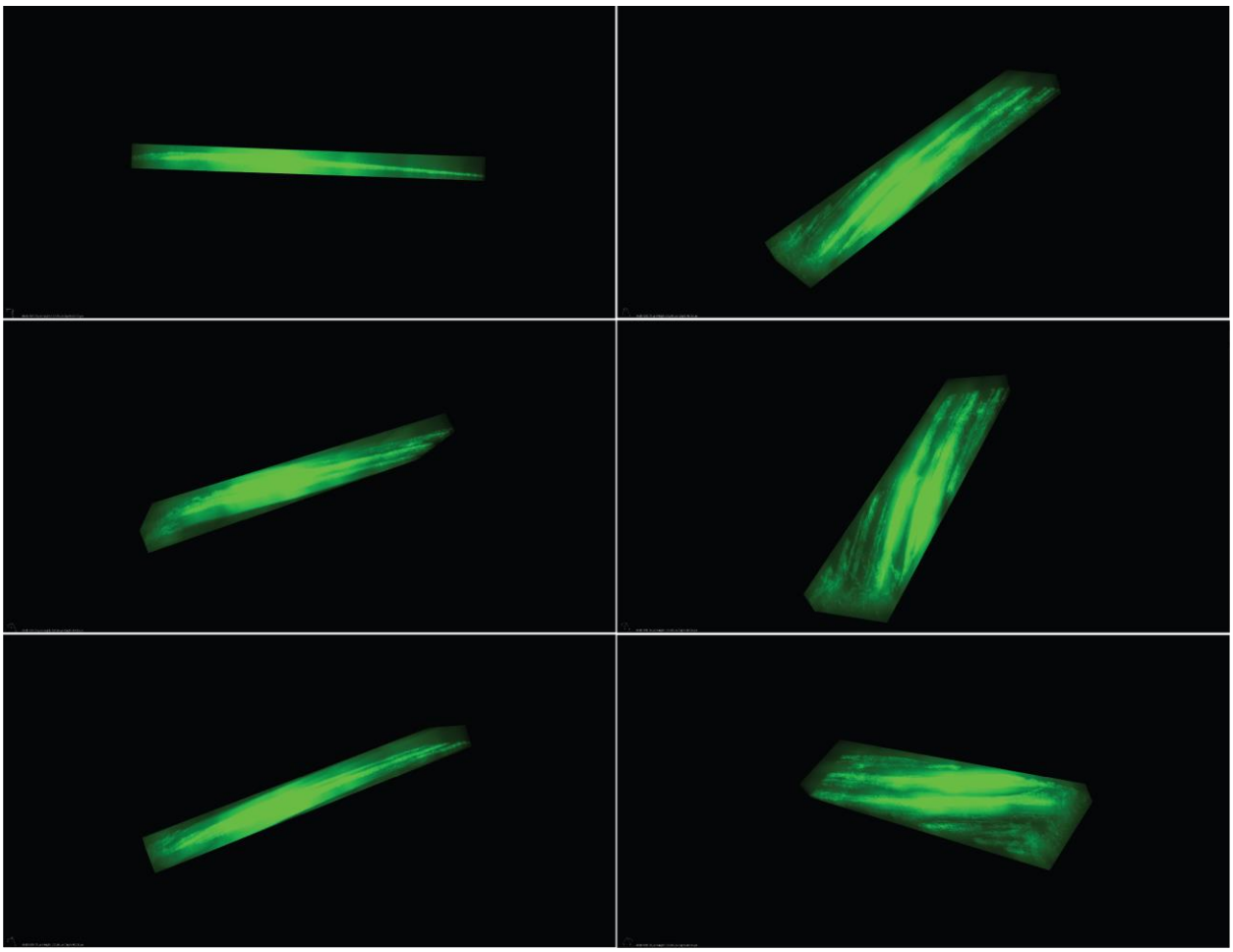

Figure S29. Confocal microscopy images of biofilm, Related to Figure 3. Confocal microscopy images showing a 3D view of biofilm (shown in Figure 3F) grown for 24 hours. Only green channel shown. Biofilm was grown for 24 hours from a 1:10 mixture of cells containing GFP (green) and mScarlet (red) on cover glass, using method depicted in Figure 2C (STAR Methods).

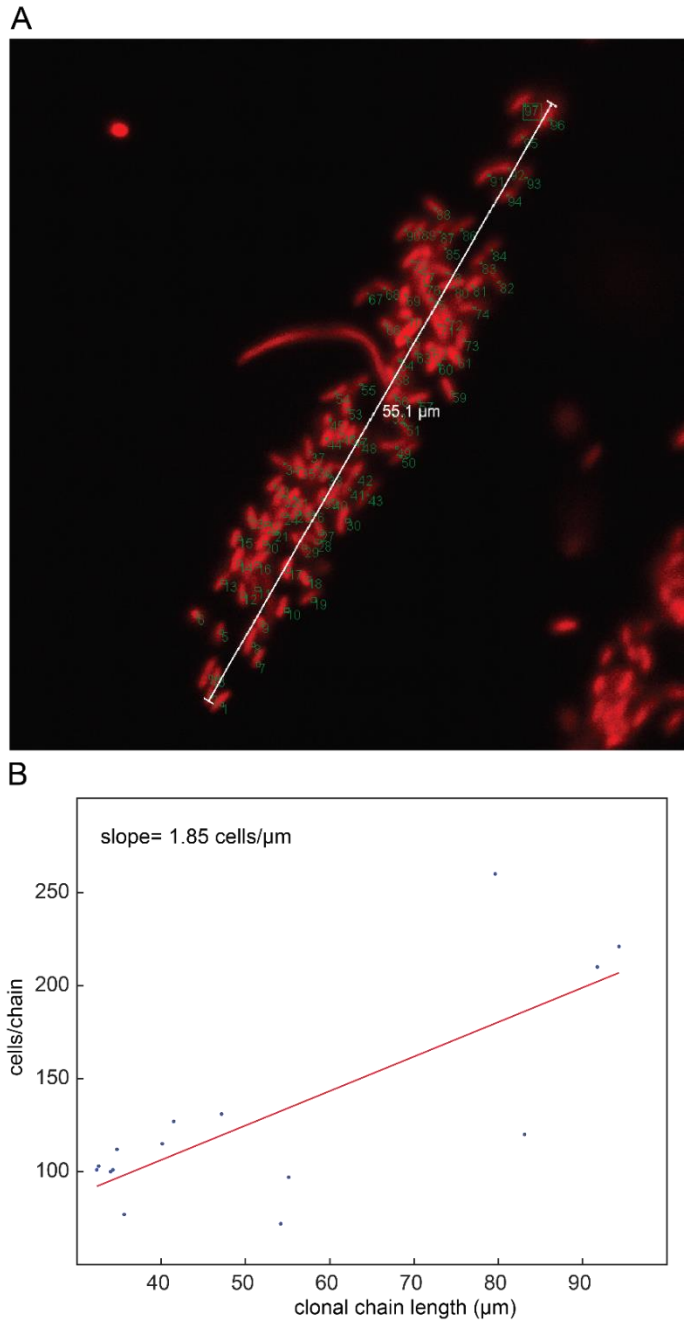

Figure S30. Characterization of clonal communities washed off of biofilms, Related to Figure 3. Biofilms grown from a 1:10 mixture of cells containing GFP (green) and mScarlet (red) on cover glass (depicted in Figure 2C; STAR Methods) were washed with phosphate-buffered saline (PBS). Run-off, collected on PBS agarose pads, contained single-color (clonal) communities (see Figures 3H-J). **(A)** Illustration of number of cells per clonal chain length. **(B)** Plot for number of cells in recovered clonal communities as a function of community length. Red line indicates fit for data. Slope calculated from fit parameters: 1.85 cells/µm; R^2: 0.6.

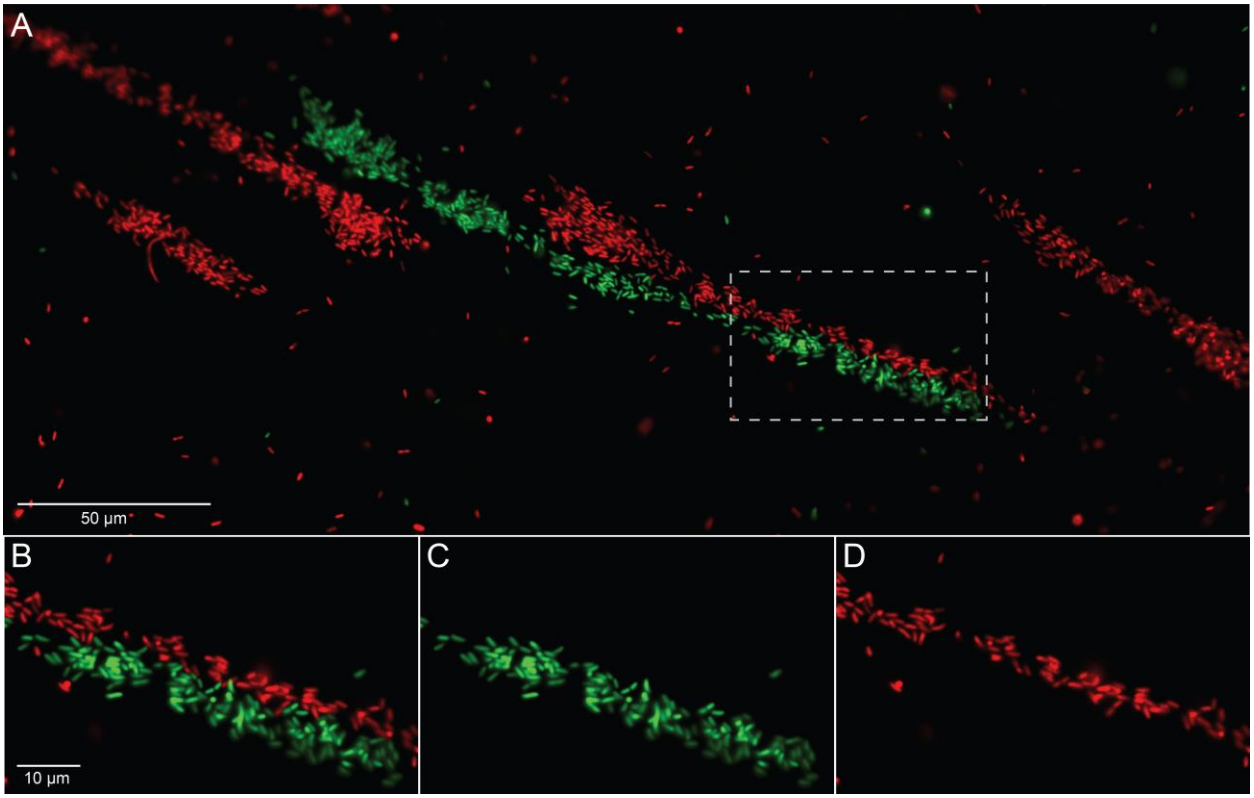

Figure S31. Illustration of clonal communities washed off of biofilms, Related to Figure 3. Biofilms grown from a 1:10 mixture of cells containing GFP (green) and mScarlet (red) on cover glass (using method depicted in Figure 2C; STAR Methods), were washed with phosphate-buffered saline (PBS). Run-off, collected on PBS agarose pads, contained single-color (clonal) communities (see also Figures 3H-J and S30; STAR Methods). **(A)** We also observed that chains could be preferentially attached to each other, as depicted by the attached red and green clonal communities recovered from the run-off of washed biofilms. Highlighted region is magnified in **(B)**. Separate **(C)** green and **(D)** red channel images from (B). Scale is indicated on micrographs.

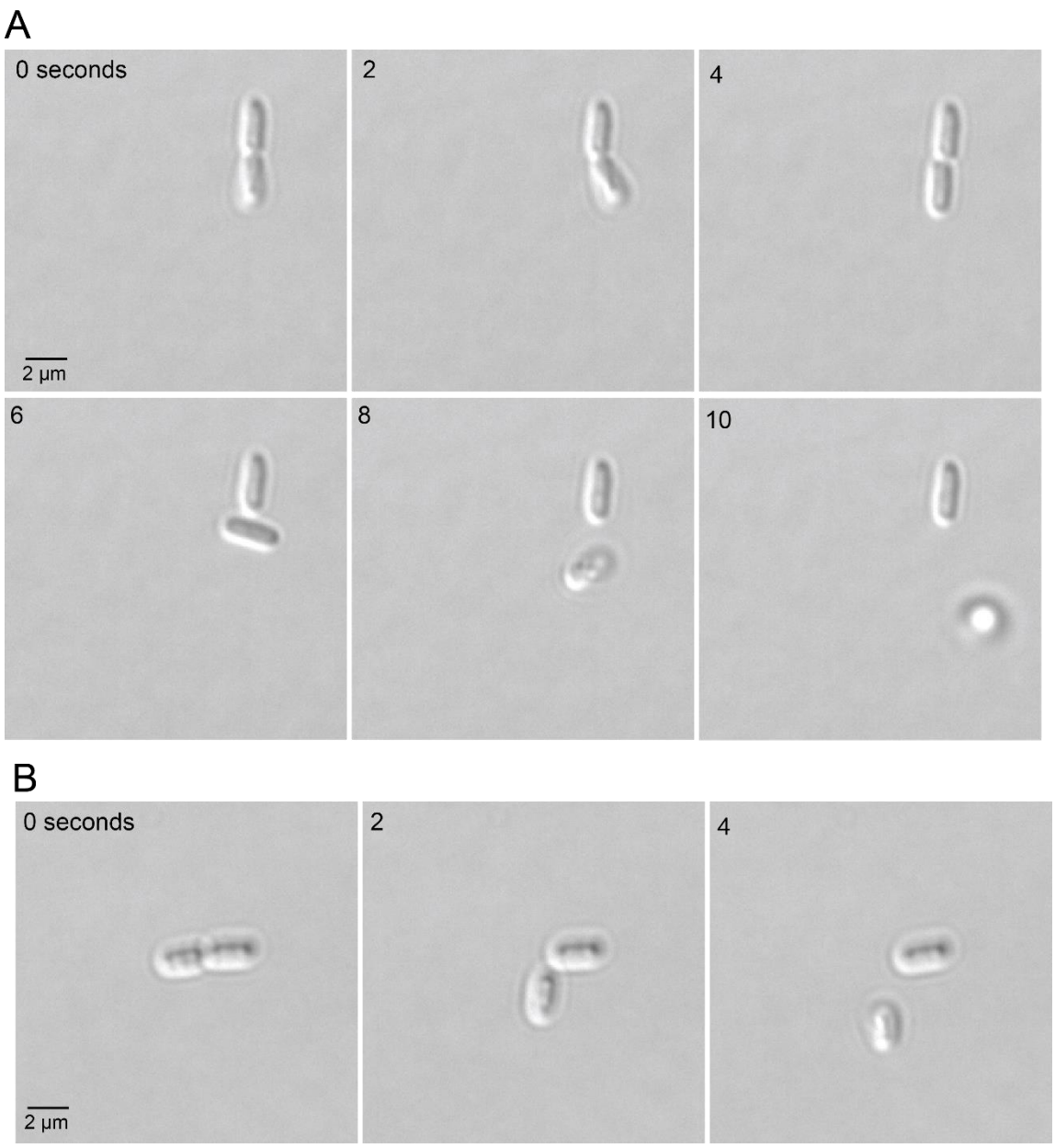

Figure S32. Sister cell separation in Δ*flu* cells, Related to Figure 4. Exponential phase cells, grown in LB media, were loaded into microfluidic device set-up depicted in Figure S1 (STAR Methods). Morphogenesis was tracked at 2-second resolution. Time and scale are indicated on micrographs.

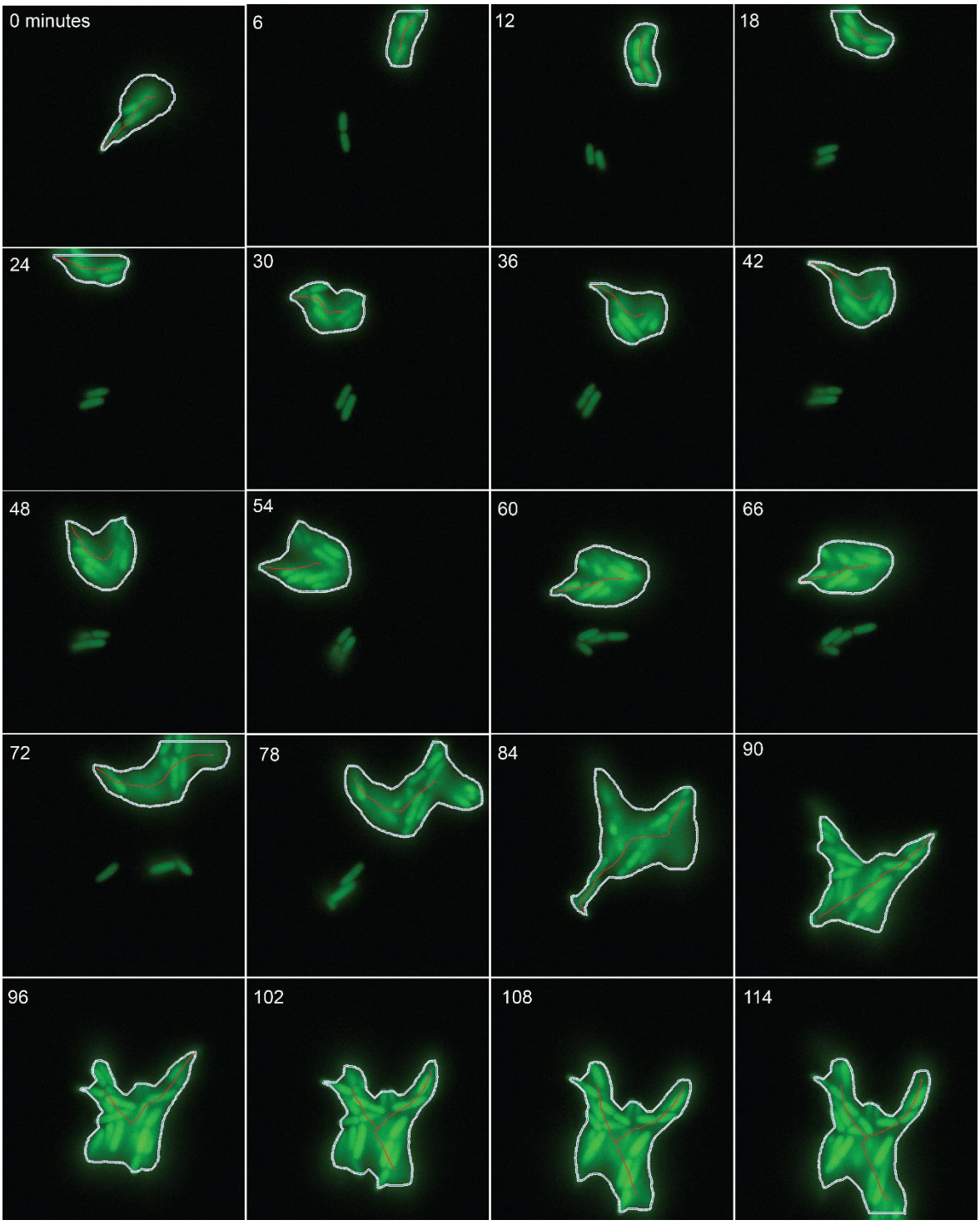

Figure S33. Illustrative example of morphogenesis in Δ*fimH* cells containing GFP, Related to Figure 4. Centerlines and boundaries are overlaid on GFP data. Exponential phase cells, grown in LB media, were loaded into microfluidic device set-up depicted in Figure S1 (STAR Methods). Micrographs show relative time. Morphogenesis was tracked every 6 minutes.

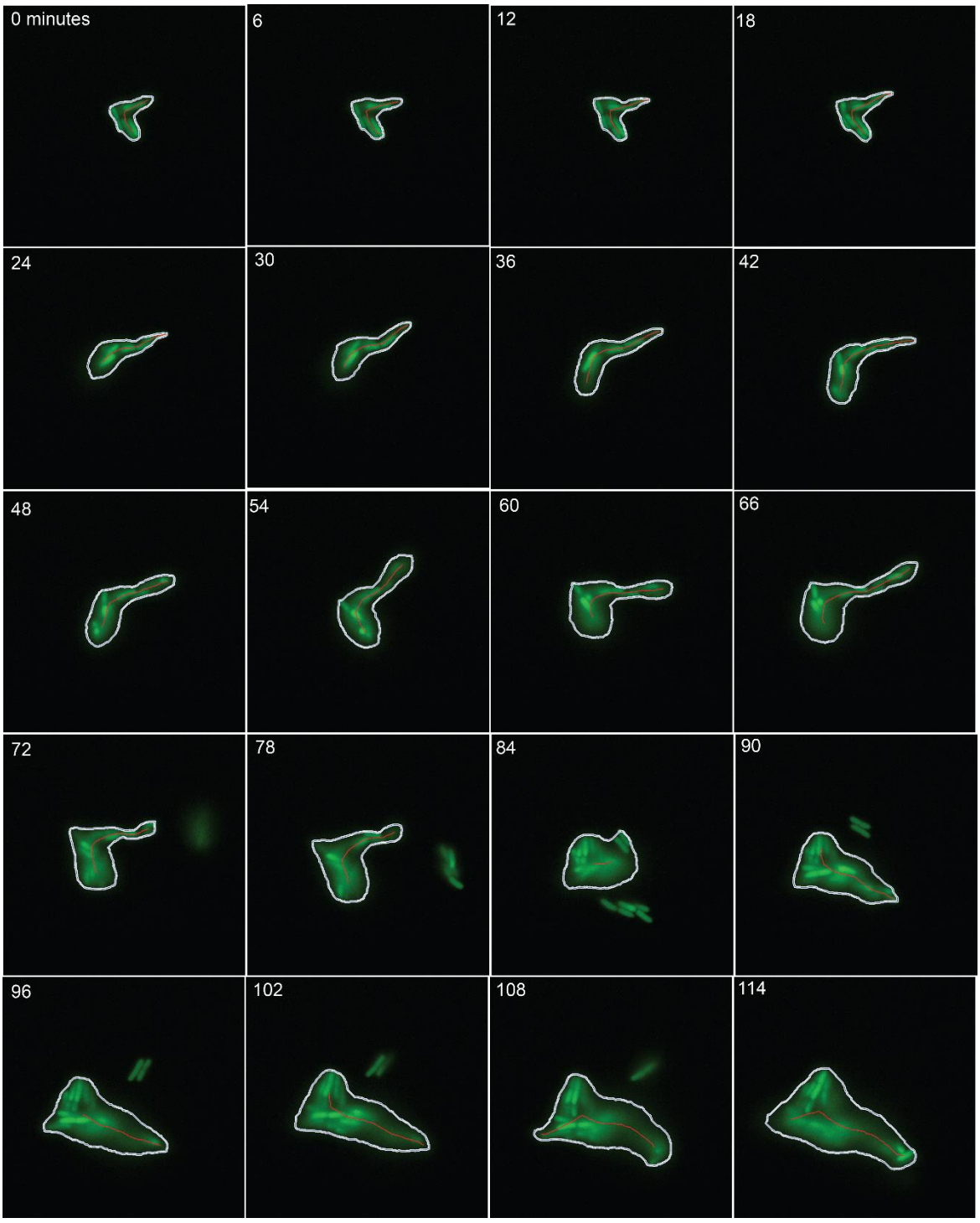

Figure S34. Illustrative example of morphogenesis in Δ*fimH* cells containing GFP, Related to Figure 4. Centerlines and boundaries are overlaid on GFP data. Exponential phase cells, grown in LB media, were loaded into microfluidic device set-up depicted in Figure S1 (STAR Methods). Micrographs show relative time. Morphogenesis was tracked every 6 minutes.

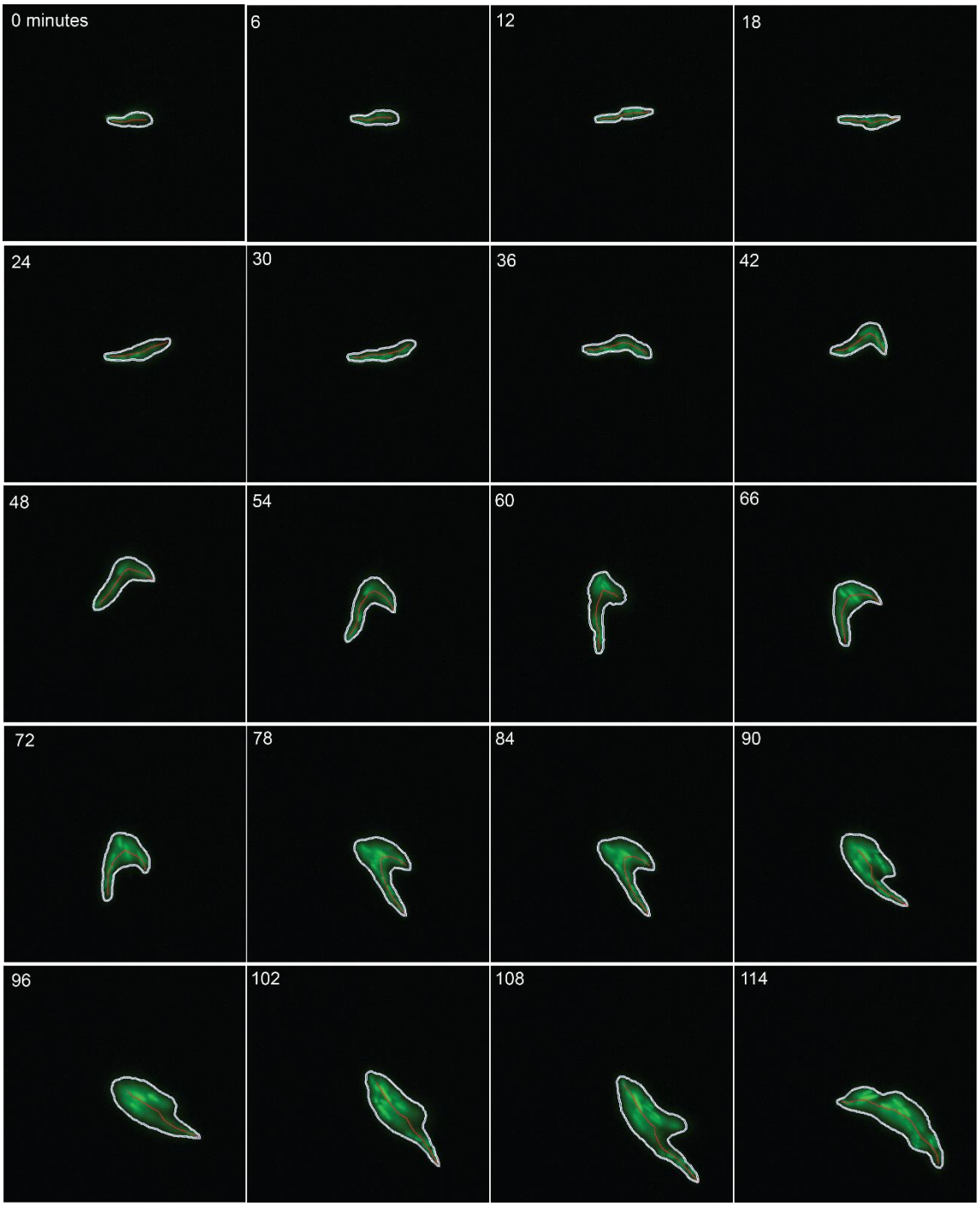

Figure S35. Illustrative example of morphogenesis in Δ*fimH* cells containing GFP, Related to Figure 4. Centerlines and boundaries are overlaid on GFP data. Exponential phase cells, grown in LB media, were loaded into microfluidic device set-up depicted in Figure S1 (STAR Methods). Micrographs show relative time. Morphogenesis was tracked every 6 minutes.

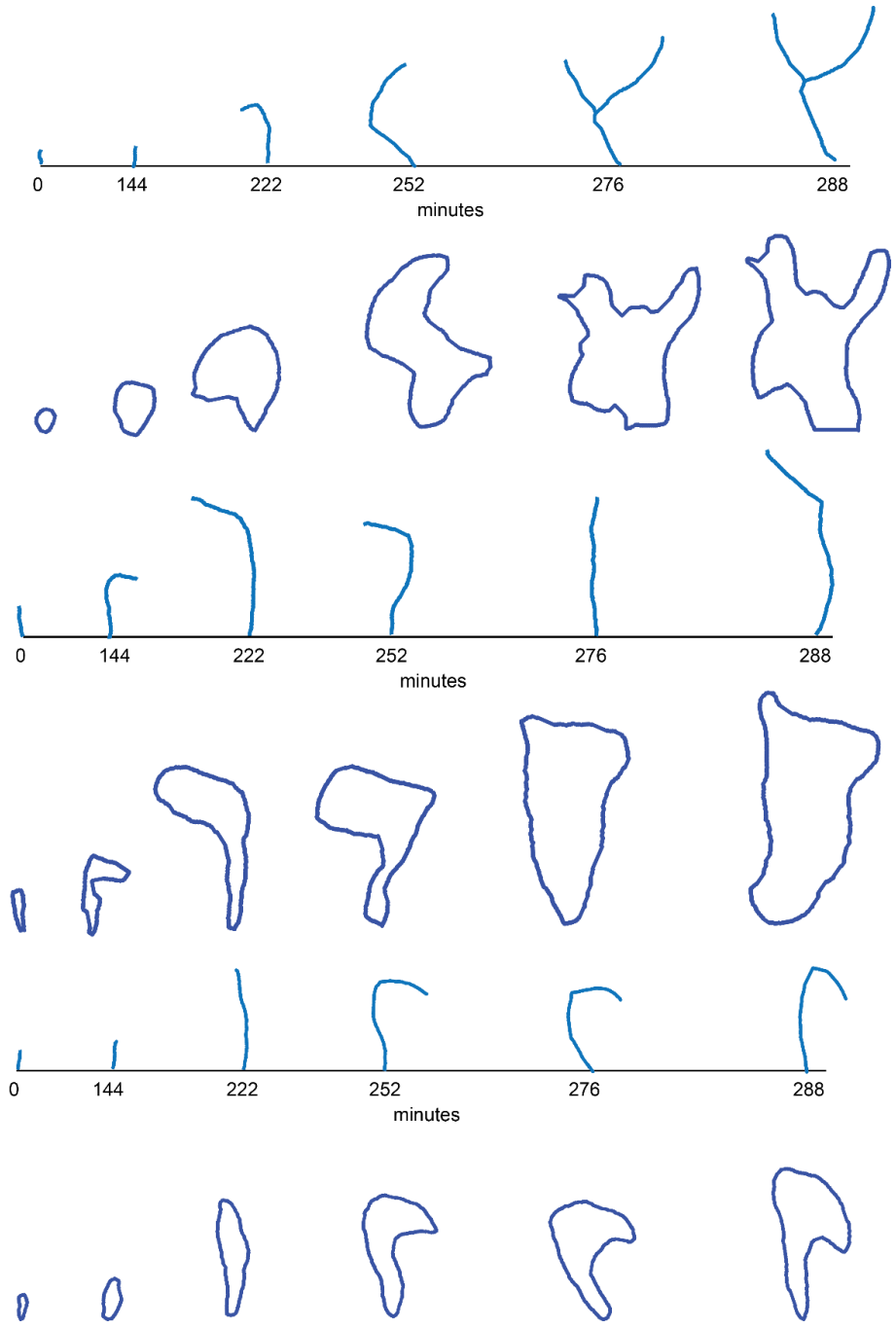

Figure S36. Centerlines and boundaries during morphogenesis in Δ*fimH* cells, Related to Figure 4. Centerlines (top panel) and boundaries (bottom panel) during morphogenesis in Δ*fimH* cells for 3 separate trajectories.

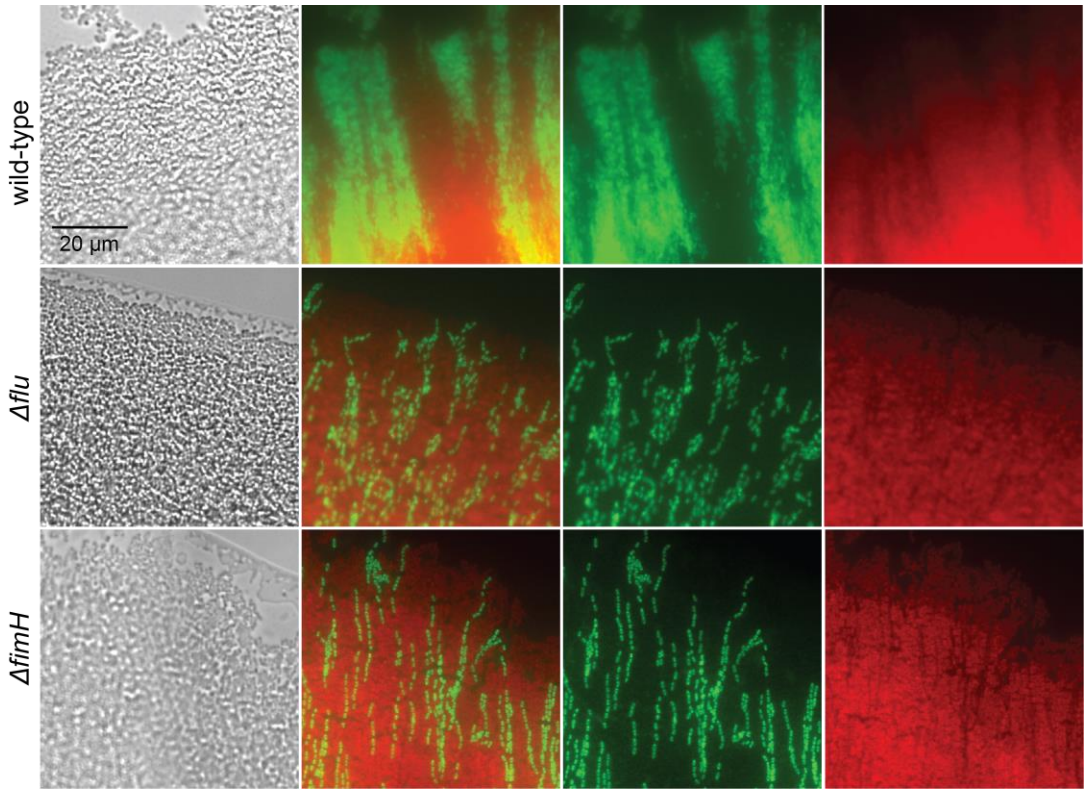

Figure S37. Cellular chain organization in wild-type, Δ*flu*, and Δ*fimH* biofilms, Related to Figure 4. Cellular chain organization in biofilms of (panel 1) wild-type, (panel 2) Δ*flu*, and (panel 3) Δ*fimH* cells (see also Figure 4). Biofilms were grown from a 1:10 mixture of cells containing GFP (green) and mScarlet (red) on cover glass, using method depicted in Figure 2C (STAR Methods). Columns 1-4 represent bright field (DIC), multi-fluorescence overlay, green fluorescence channel, and red fluorescence channel, respectively. Micrographs represent XY imaging plane. Scale is indicated on micrographs.

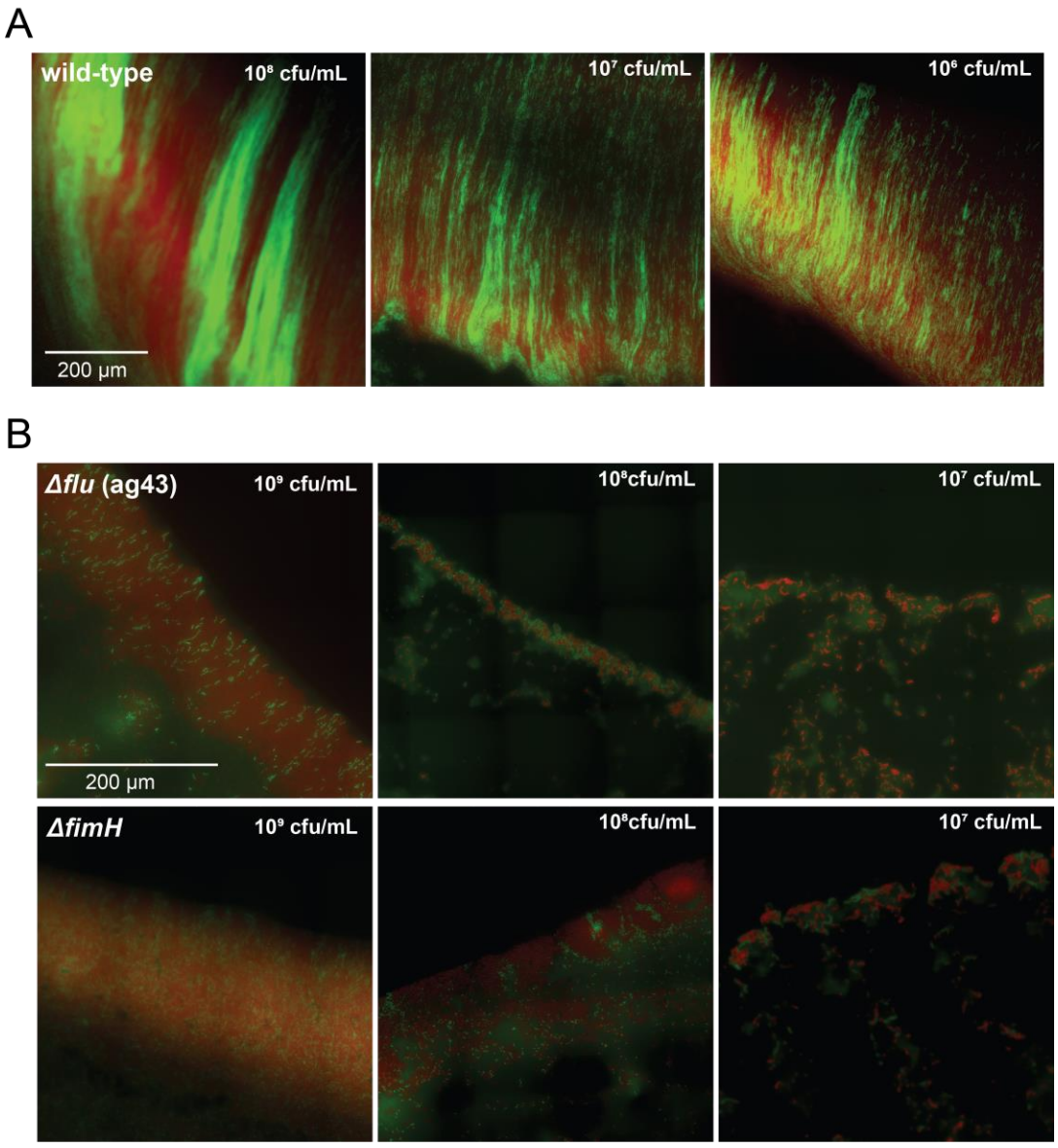

Figure S38. Wild-type, Δ*flu*, and Δ*fimH* biofilms with diluted inoculum, Related to Figure 5. **(A)** Wild-type biofilms with diluted inoculum (a 1:10 mixture of cells containing GFP (green) and mScarlet (red)) was used to inoculate the biofilm using method depicted in Figure 2C (STAR Methods). Panels 1-3 represent 10^8, 10^7, and 10^6 cfu/mL inoculum respectively. **(B)** Δ*flu* and Δ*fimH* biofilms with diluted inoculum. Panels 1-3 represent 10^9, 10^8, and 10^7 cfu/mL inoculum respectively. Micrographs represent XY imaging plane. Scale is indicated on micrographs.

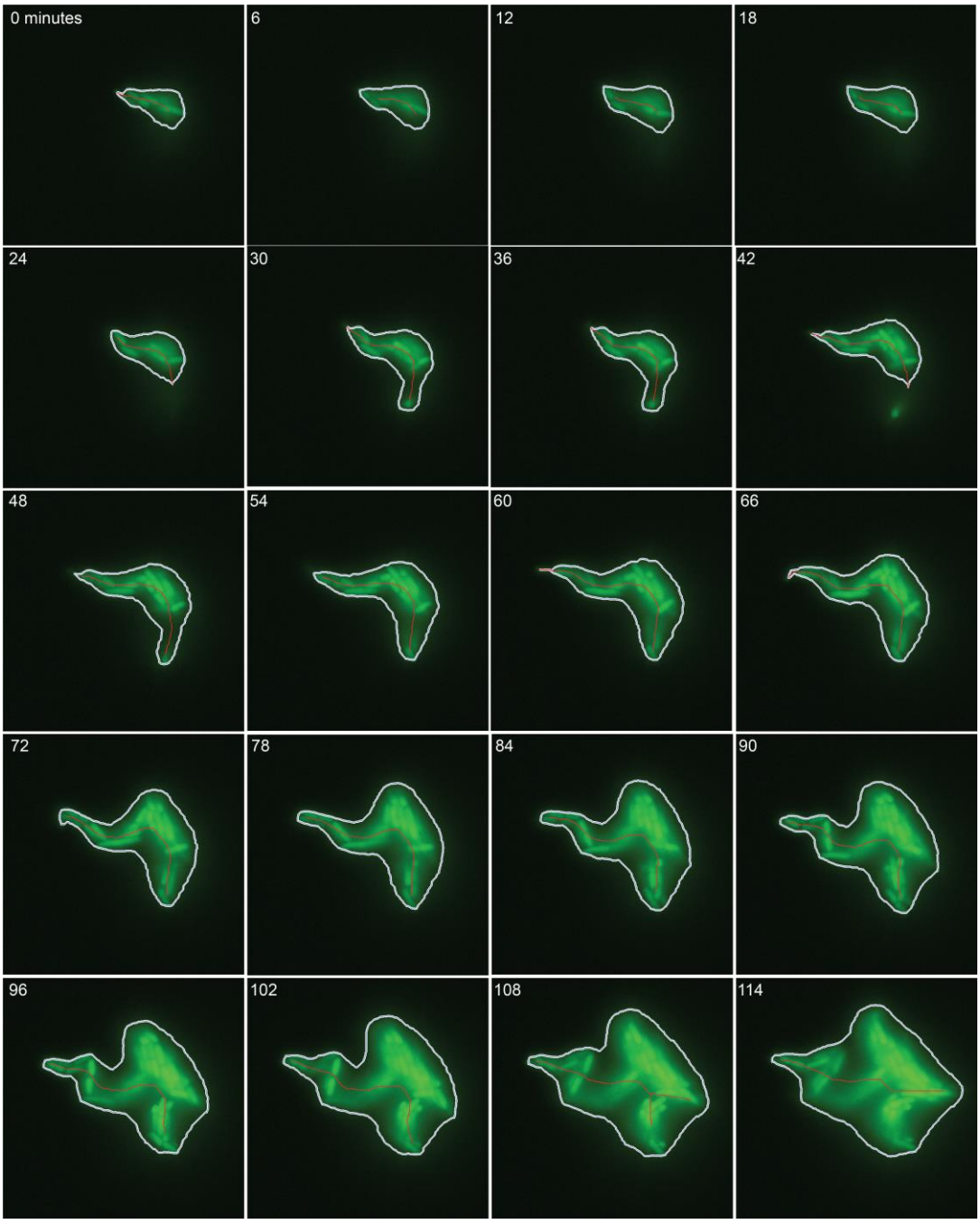

Figure S39. Illustrative example of morphogenesis in Δ*csgA* cells containing GFP, Related to Figure 6. Centerlines and boundaries are overlaid on GFP data. Exponential phase cells, grown in LB media, were loaded into microfluidic device set-up depicted in Figure S1 (STAR Methods). Micrographs show relative time. Morphogenesis was tracked every 6 minutes.

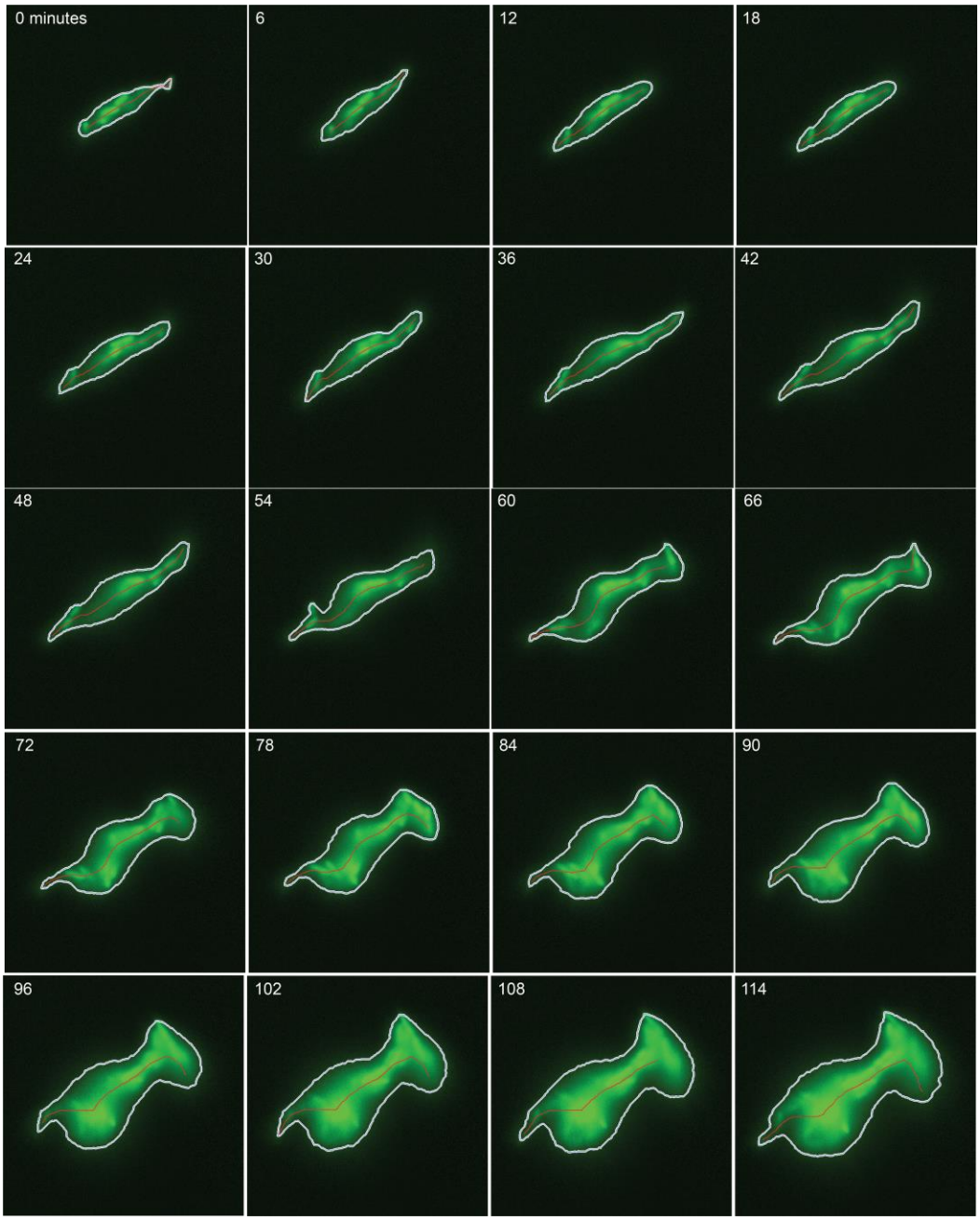

Figure S40. Illustrative example of morphogenesis in Δ*csgA* cells containing GFP, Related to Figure 6. Centerlines and boundaries are overlaid on GFP data. Exponential phase cells, grown in LB media, were loaded into microfluidic device set-up depicted in Figure S1 (STAR Methods). Micrographs show relative time. Morphogenesis was tracked every 6 minutes.

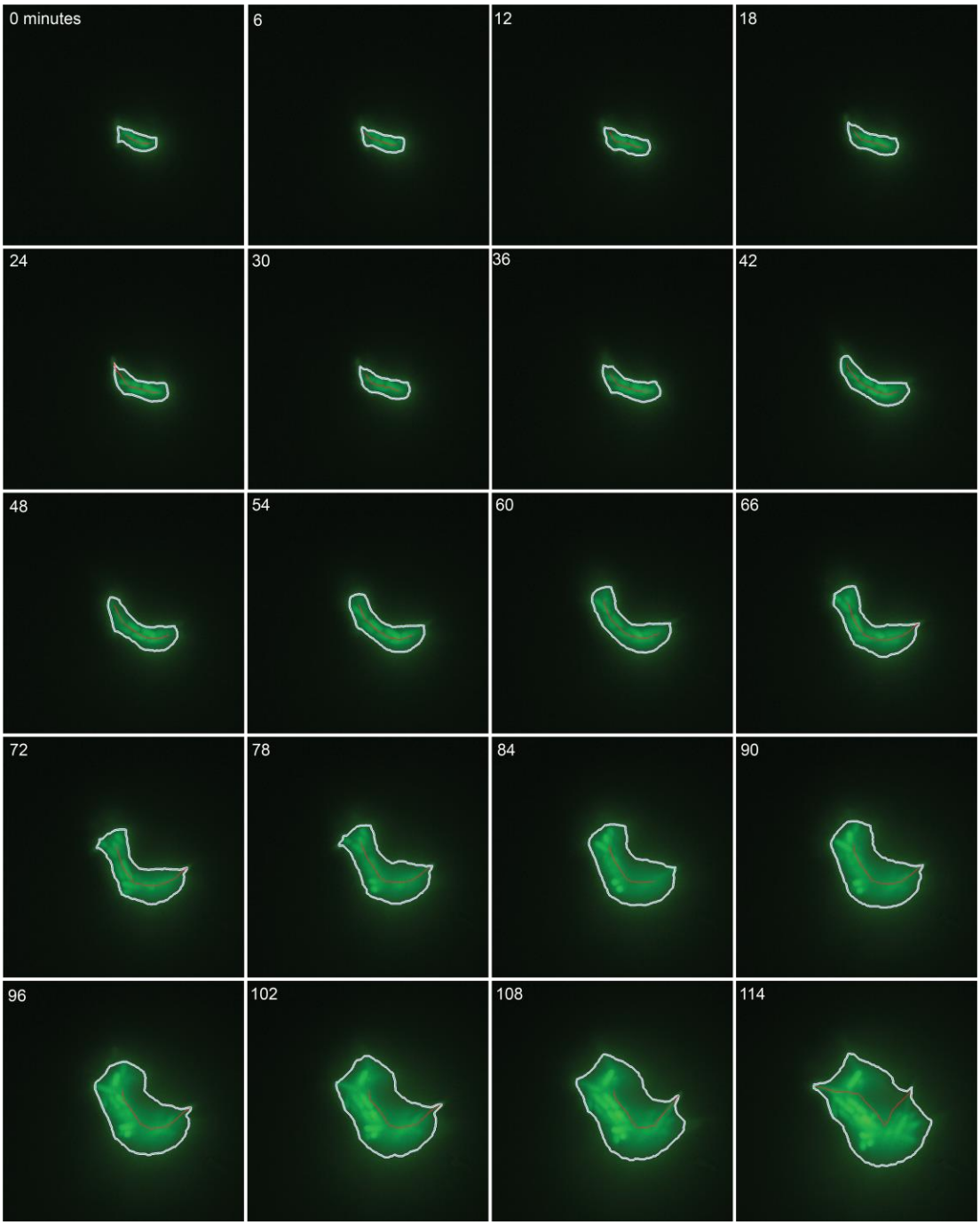

Figure S41. Illustrative example of morphogenesis in Δ*csgA* cells containing GFP, Related to Figure 6. Centerlines and boundaries are overlaid on GFP data. Exponential phase cells, grown in LB media, were loaded into microfluidic device set-up depicted in Figure S1 (STAR Methods). Micrographs show relative time. Morphogenesis was tracked every 6 minutes.

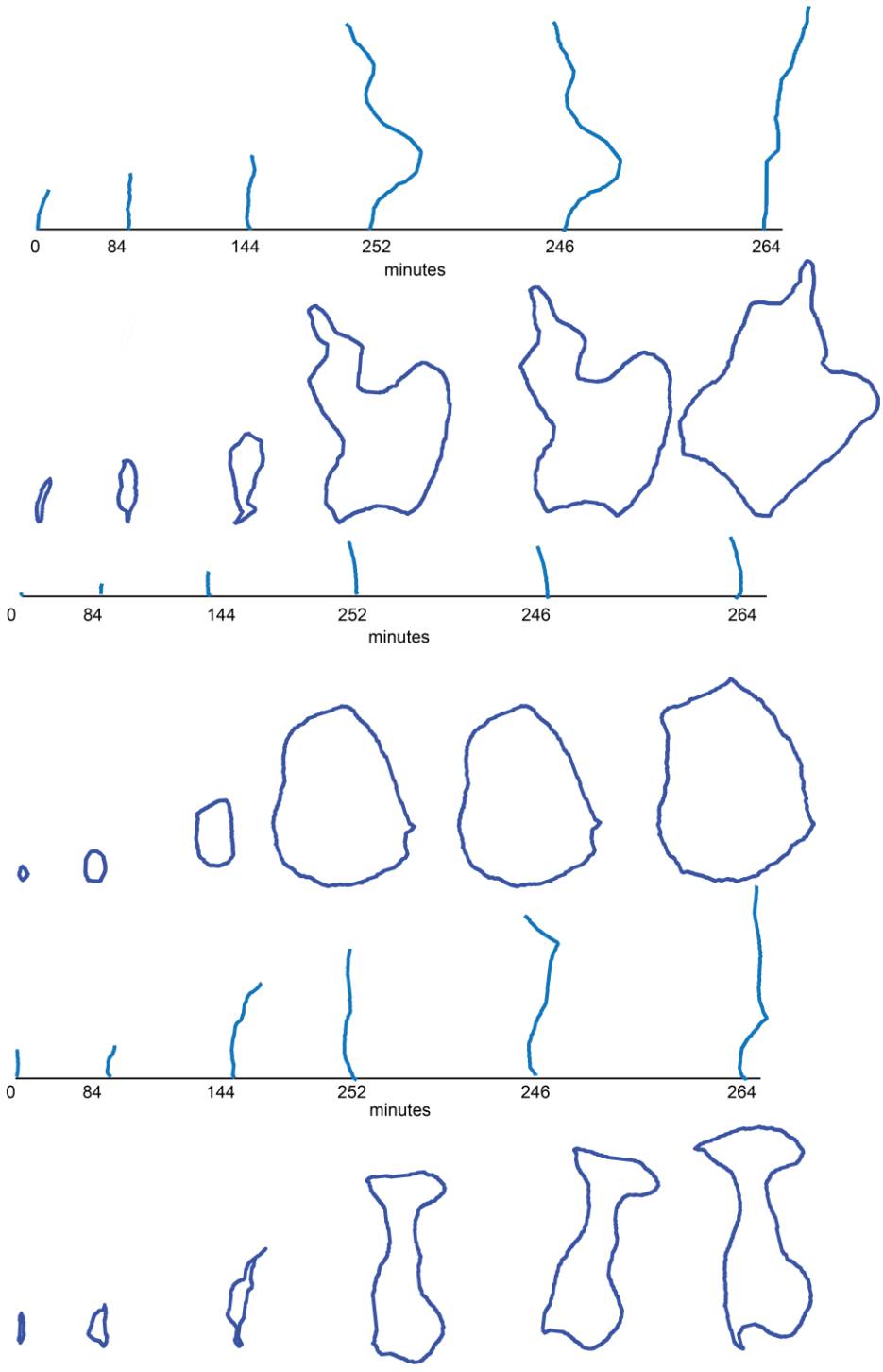

Figure S42. Centerlines and boundaries during morphogenesis in Δ*csgA* cells, Related to Figure 6. Centerlines (top panel) and boundaries (bottom panel) during morphogenesis in Δ*csgA* cells for 3 separate trajectories.

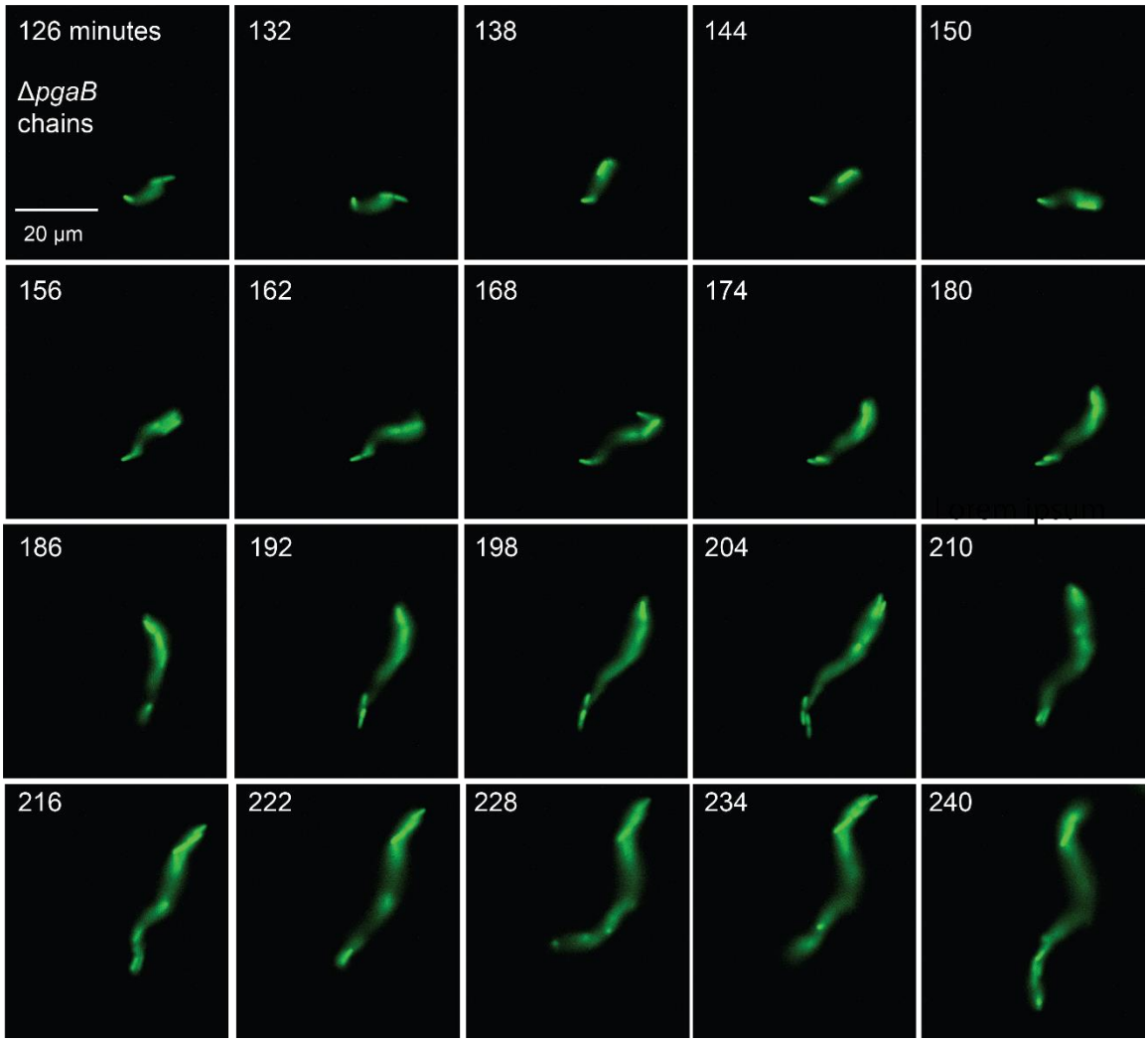

Figure S43. Illustrative example of early stages of morphogenesis in Δ*pgaB* cells containing GFP, Related to Figure 6. Exponential phase cells, grown in LB media, were loaded into microfluidic device set-up depicted in Figure S1 (STAR Methods). Morphogenesis was tracked every 6 minutes. Time and scale are indicated on micrographs.

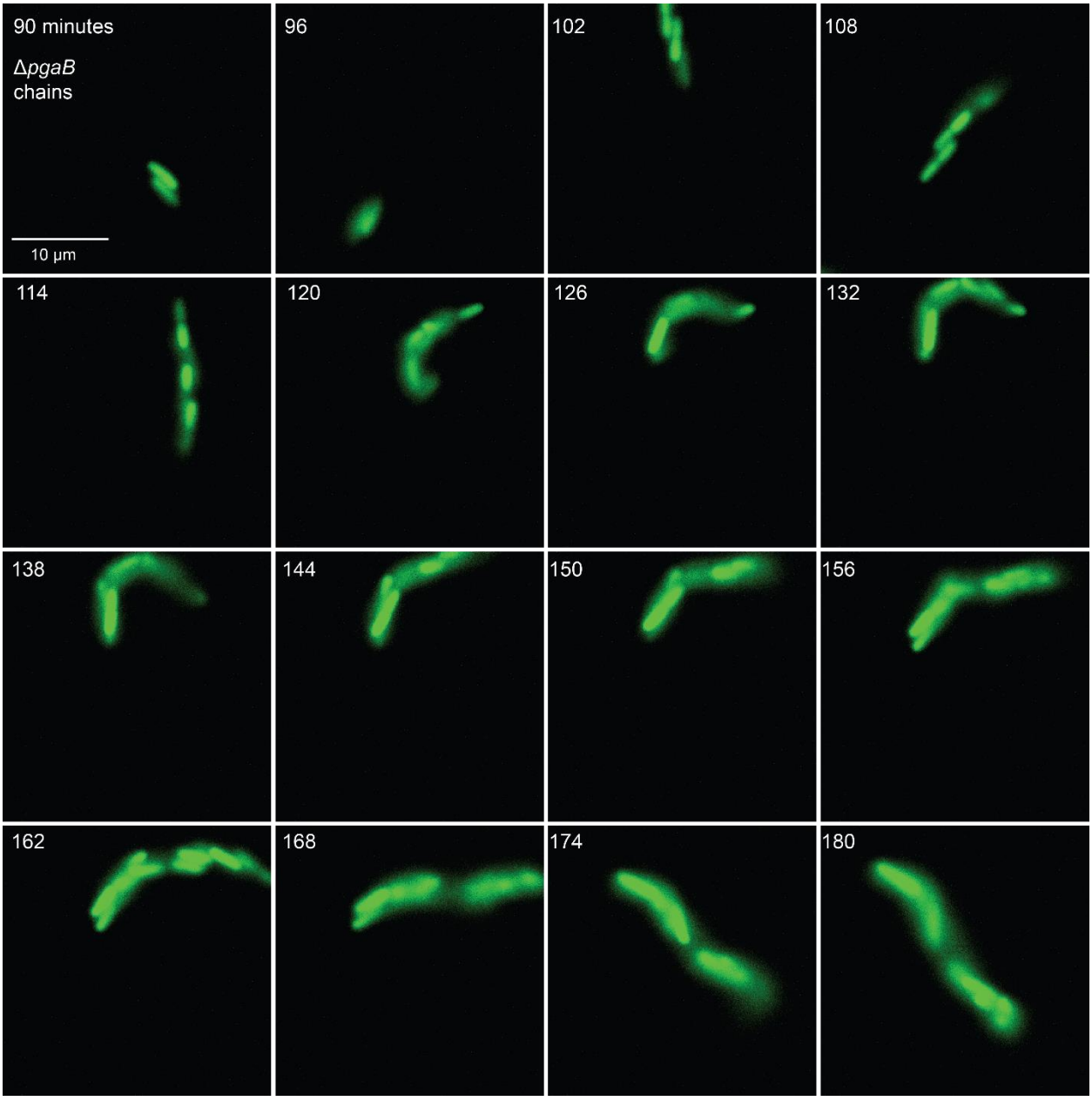

Figure S44. Illustrative example of early stages of morphogenesis in Δ*pgaB* cells containing GFP, Related to Figure 6. Exponential phase cells, grown in LB media, were loaded into microfluidic device set-up depicted in Figure S1 (STAR Methods). Morphogenesis was tracked every 6 minutes. Time and scale are indicated on micrographs.

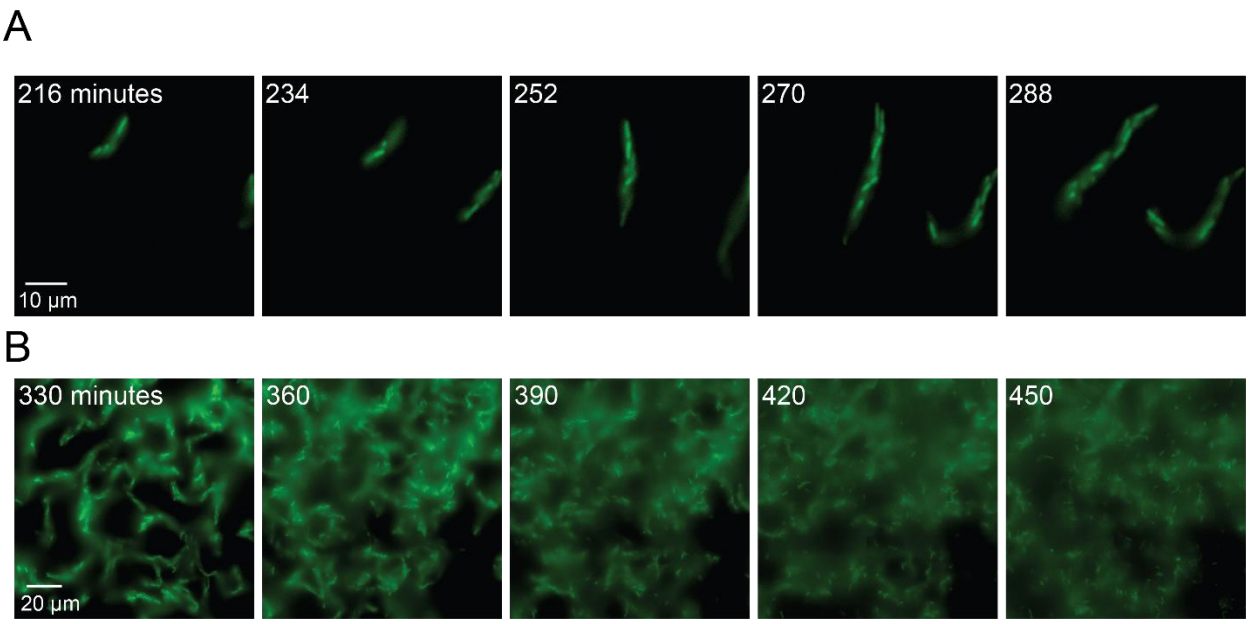

Figure S45. Early and late stages of morphogenesis in Δ*pgaB* cells, Related to Figure 6. Illustrative example of **(A)** early stages and **(B)** late stages of morphogenesis in Δ*pgaB* cells containing GFP. Exponential phase cells, grown in LB media, were loaded into microfluidic device set-up depicted in Figure S1 (STAR Methods). Morphogenesis was tracked every 6 minutes. Time and scale are indicated on micrographs.

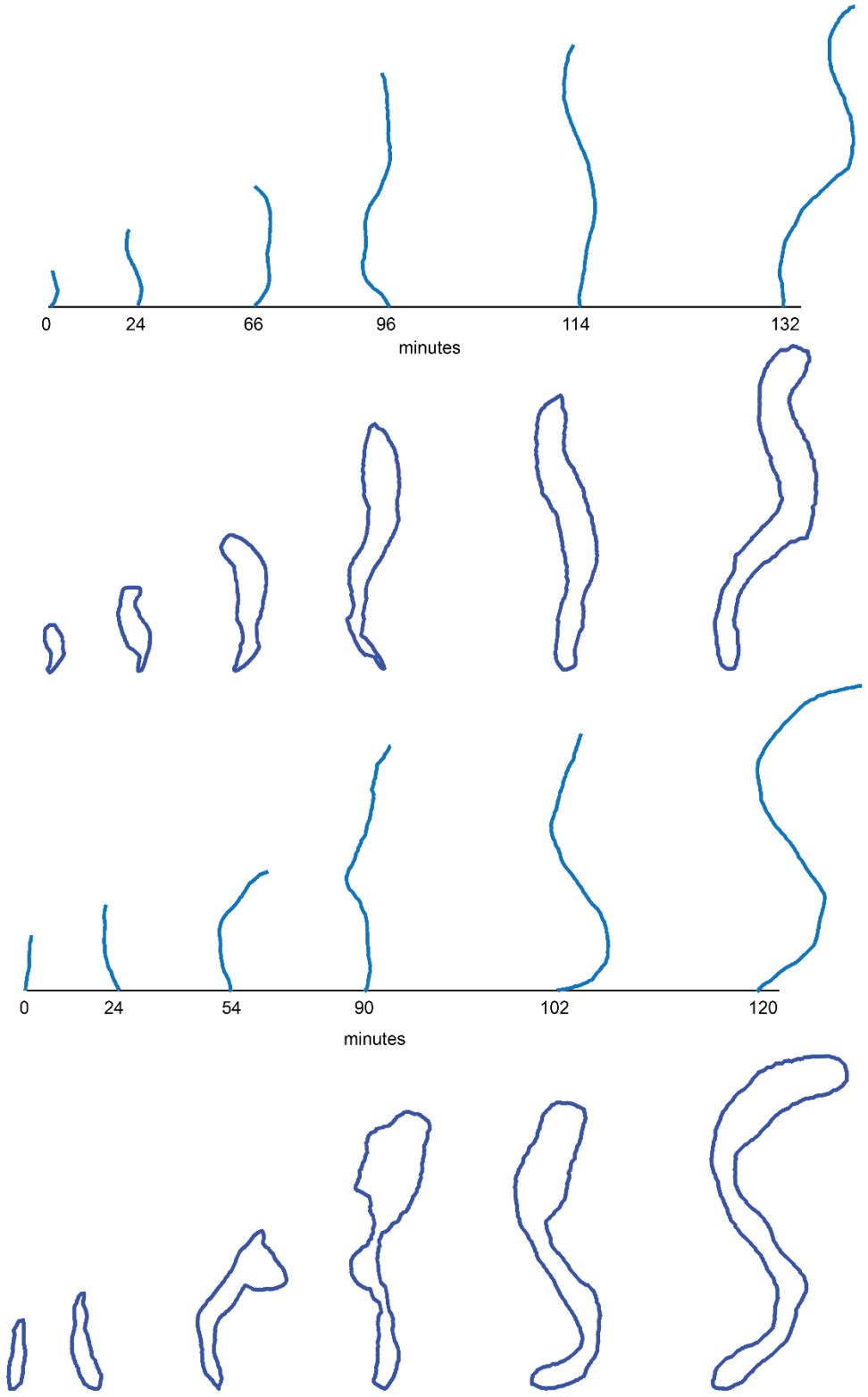

Figure S46. Centerlines and boundaries during morphogenesis in Δ*pgaB* cells, Related to Figure 6. Centerlines (top panel) and boundaries (bottom panel) during morphogenesis in Δ*pgaB* cells for 2 separate trajectories.

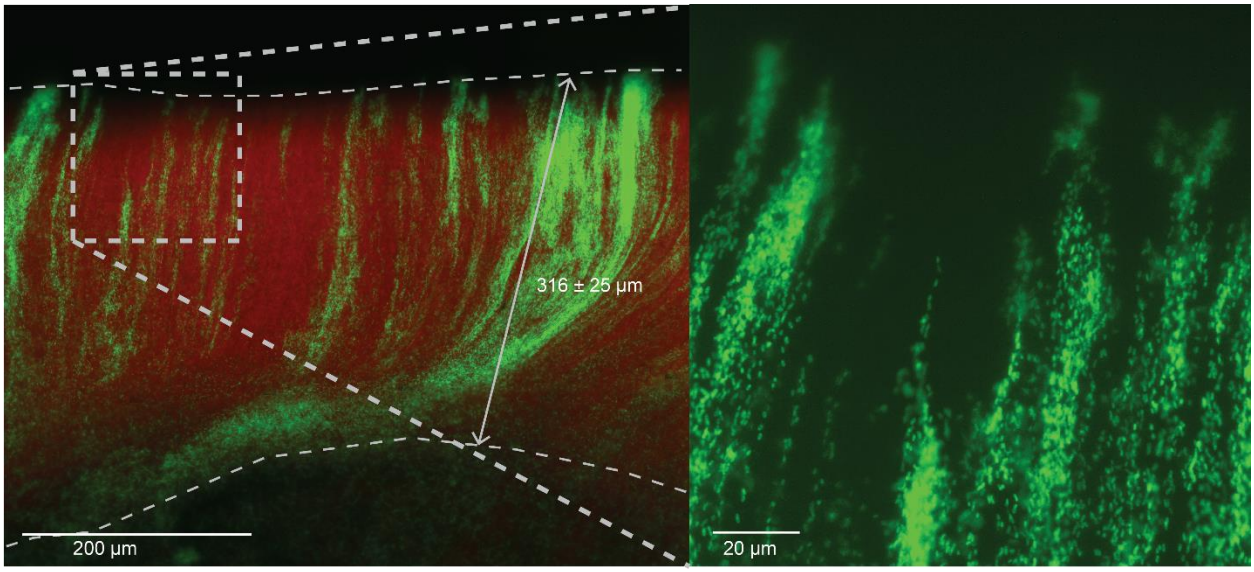

Figure S47. ***E. coli*** **BW25113 biofilm consisting of clonal chains**, Related to Figure 7. Biofilms were grown from a 1:10 mixture of cells containing GFP (green) and mScarlet (red) on cover glass using method depicted in Figure 2C (STAR Methods). Highlighted region is magnified on the right panel (only green fluorescence shown). Micrographs represent XY imaging plane. Scale and biofilm depth indicated on micrograph.

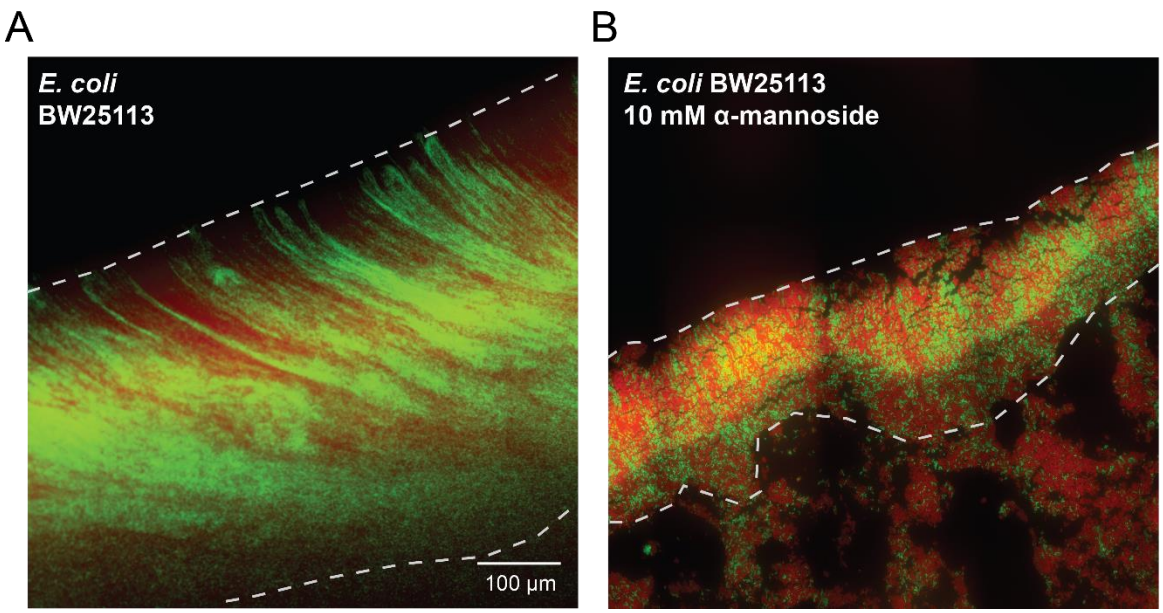

Figure S48. ***E. coli*** **BW25113 biofilms grown with mannoside**, Related to Figure 7. *E. coli* BW25113 biofilms grown without **(A)** or with **(B)** 10 mM mannoside. Biofilms were grown from a 1:10 mixture of cells containing GFP (green) and mScarlet (red) on cover glass using method depicted in Figure 2C (STAR Methods). Micrographs represent XY imaging plane. Scale is indicated on micrograph.

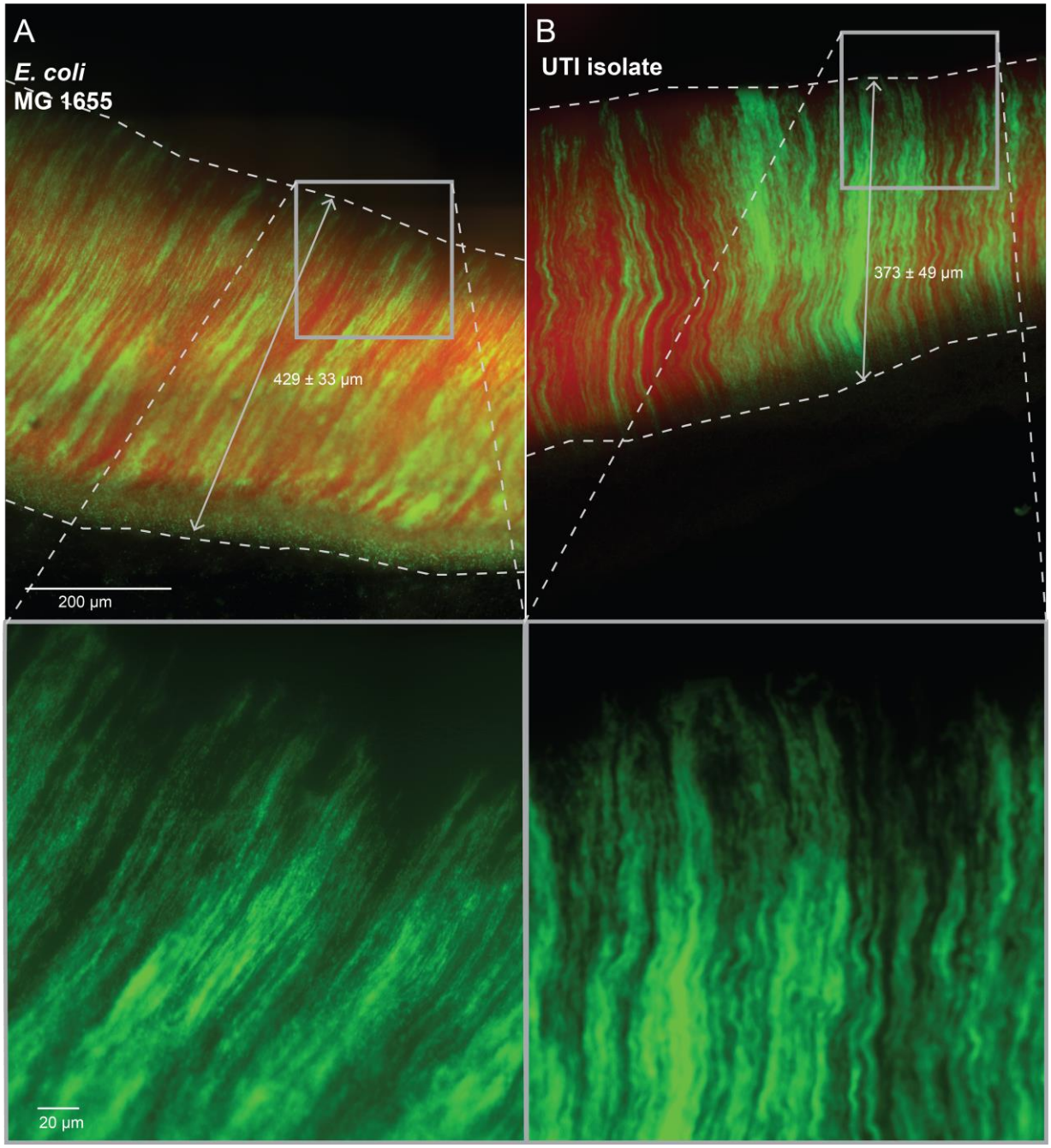

Figure S49. Comparison of biofilm assembled by *E. coli* strains MG1655 and UTI isolate, Related to Figure 7. Biofilm assembled by *E. coli* strains **(A)** MG1655 and **(B)** UTI isolate. Biofilms were grown from a 1:10 mixture of cells containing GFP (green) and mScarlet (red) on cover glass using method depicted in Figure 2C (STAR Methods). Highlighted regions are magnified in bottom panels (only green channel shown). Micrographs represent XY imaging plane. Scale and biofilm depth are indicated on micrographs.

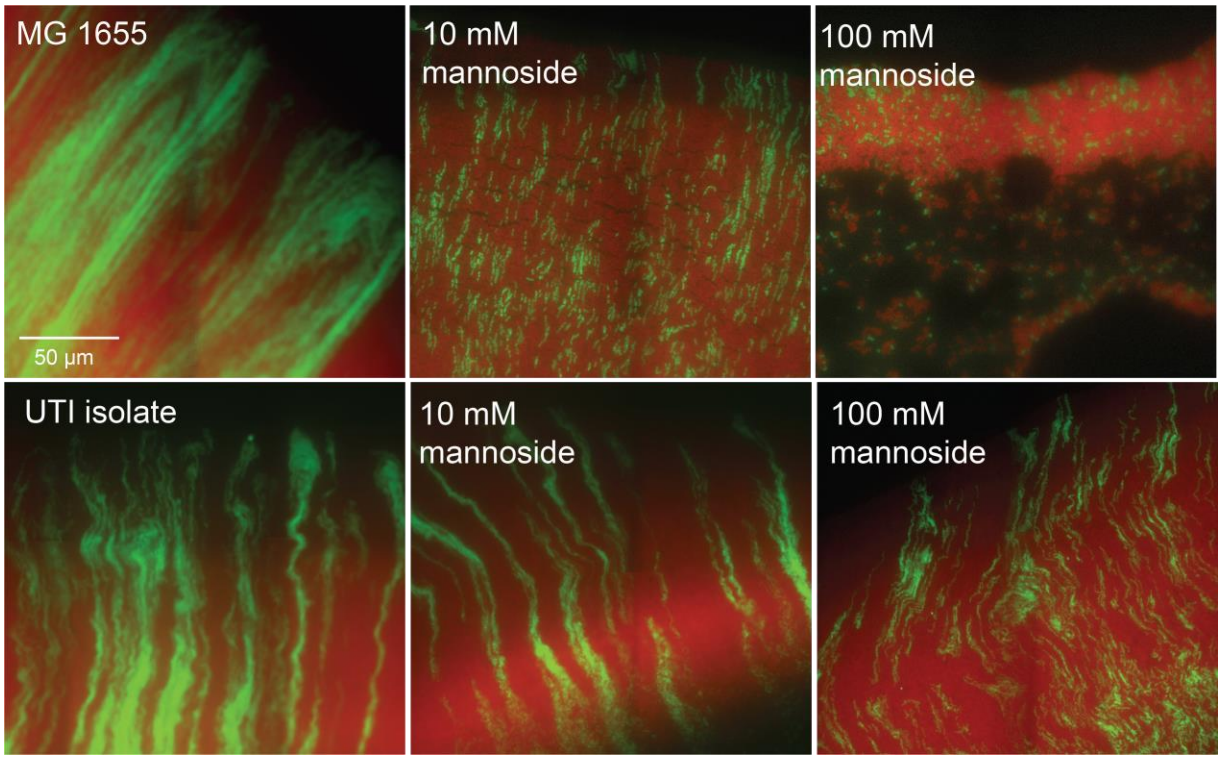

Figure S50. ***E. coli*** **MG1655 and UTI isolate biofilms grown with mannoside**, Related to Figure 7. *E. coli* MG1655 and (bottom panel) UTI isolate biofilms grown with 0, 10, and 100 mM of mannoside. Biofilms were grown from a 1:10 mixture of cells containing GFP (green) and mScarlet (red) on cover glass using method depicted in Figure 2C (STAR Methods). Addition of 10 mM mannoside disrupted chain structures in MG1655 biofilms, whereas UTI isolate biofilms required a higher mannoside concentration (100 mM) for chains to be disrupted. Micrographs represent XY imaging plane. Scale is indicated on micrographs.

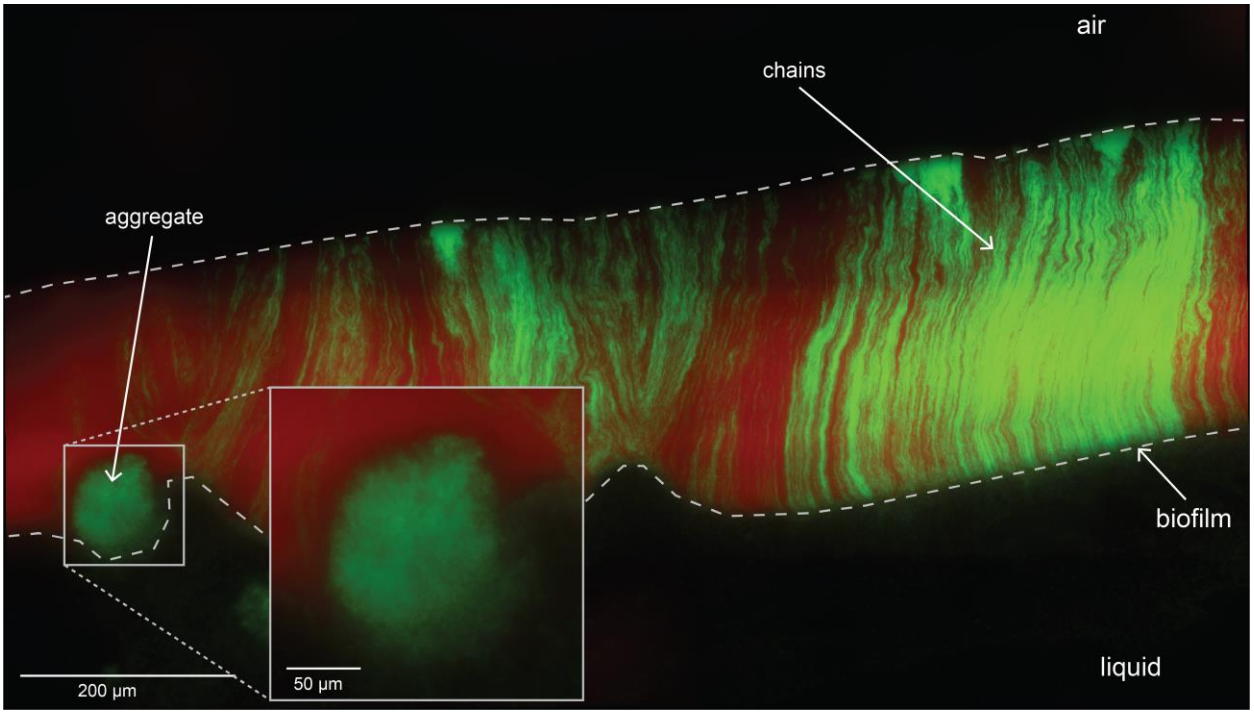

Figure S51. Biofilms assembled by UTI isolate, Related to Figure 7. Biofilms assembled by UTI isolate consisting of clonal cellular chains. In rare cases, clonal aggregates were also observed in UTI isolate biofilms. Biofilms were grown from a 1:10 mixture of cells containing GFP (green) and mScarlet (red) on cover glass using method depicted in Figure 2C (STAR Methods). Scale is indicated on micrographs. Highlighted region is magnified in inset.